CHARACTERIZATION OF Cu_xN_y AND CdO:Al THIN FILMS FOR SOLAR CELL APPLICATIONS

OBARE BENARD MOSOTI [B.Ed. (Sc.)]

I56/CE/22377/2010

A Thesis Submitted in Partial Fulfillment of The Requirements for The Award of The Degree of Master of Science (Electronics and Instrumentation) in The School of Pure and Applied Sciences of Kenyatta University

MAY 2016

DECLARATION

This thesis is my original work and has not been presented for the award of any degree or any other award in any university.

Obare Benard Mosoti Signature..... Date.....18/5/2016

(I56/CE/22377/2010)

Department of Physics

Kenyatta University

This thesis has been submitted for examination with our approval as university supervisors

Dr. W.K. NJOROGE Signature..... Date...18/05/2016

Department of Physics

Kenyatta University

Dr. M. K. MUNJI Signature..... Date.....18/05/2016

Department of Physics

Kenyatta University

DEDICATION

This thesis is a dedication to my parents; Samuel Obare and Priscah Nyaboke, beloved wife Everline Nyaboke and my two daughters; Mitchelle and Charlene.

ACKNOWLEDGEMENTS

First, I thank God for the tender care He has taken over me during the pursuance of this course. He has enabled me to accomplish this much. May the honor and Glory be to Him.

Secondly, I express my gratitude to my research supervisors Dr. Walter K. Njoroge and Dr. Mathew Munji who worked tirelessly in guiding me throughout the research process. I owe the successful completion of the research to them especially their unreserved attention they gave for consultations. Their immense knowledge and wisdom was of great input to this work. I truly acknowledge and appreciate their efforts in showing me the way forward whenever I was challenged.

Also, I recognize the department of Physics of University of Nairobi-Chiromo campus for their equipment used in this research. These include Edwards auto 306 vacuum coater that was used in preparation of the thin films and the UV-VIS-NIR Spectrophotometer that was used to measure the optical properties of the thin films. A special appreciation goes to Mr. Bonface Muthoka, a technician in Solid State laboratory who assisted me especially in thin film preparation and carrying out measurement of optical properties. In addition, I extend my appreciation to the International Science Programme (ISP) based at Uppsala University, Sweden for their support in donating the said equipment to University of Nairobi. I also appreciate the entire technical staff of Physics Department of Kenyatta University for their support and advice, especially when doing sample preparation in the laboratory.

My sincere gratitude also goes to my Programme colleagues like Samwel Opiyo, Charles Mogunde, Wycliffe Nyaberi, Jared Ombaba, Nicholas Ososi, Paul

Onkundi, Sally Ndonye and Edward Omuga among others. Their motivation and spirit of hard work was a source of encouragement to me to carry on with research.

I also thank my parents, Mr. and Mrs. Samuel Obare for their tender care, love and support during my research period. They always encouraged me to work hard and prayed for that I come out successful. I cannot forget the part played by my brothers and sisters in reminding me about completing the course.

Many thanks to my wife Everline Nyaboke and our daughters Mitchelle Kerubo and Charlene Moraa for their moral support during pursuance of this research. They were a source of unlimited love, inspiration and motivation.

Finally, I would like to acknowledge the financial support by National Commission For Science, Technology and Innovation towards this research. It is through their support that I was able to accomplish this research.

TABLE OF CONTENTS

LIST OF TABLES

LIST OF FIGURES

ABBREVIATIONS, ACRONYMS AND SYMBOLS

Al_2O_3	Aluminium Oxide
C	Speed of light
CB	Conduction band
CdO	Cadmium Oxide
CdO:Al	Aluminium doped Cadmium Oxide
CdO:Sn	Tin doped Cadmium Oxide
CdSe	Cadmium Selenide
$CuInSe_2$	Copper Indium Selenide
Cu_3N	Copper (I) nitride
CuO	Copper Oxide
CVD	Chemical Vapor Deposition
dc	Direct current
eV	Electron volt
E_f	Fermi level
E_g	Optical energy band gap
E-H	Electron-hole
FF	Fill factor
GaAs	Gallium Arsenide
H	Planck’s constant
HEP	Hydro-electric power
In_2Se_3	Indium Selenide
I-V	Current versus voltage
ITO	Indium Tin Oxide

J_o	Dark saturation current density
J_{sc}	Short circuit current density
K	Extinction coefficient
LVD	Liquid vapor deposition
M	Molecular weight
MBE	Molecular beam epitaxy
MOCVD	Metal oxide chemical vapor deposition
N	Refractive index
NiO	Nickel oxide
P_e	Equilibrium Pressure
pn	Junction between p- and n- layers
R	Reflectance
RF	Radio frequency
Sccm	Standard cubic centimeters
SEM	Scanning electron microscope
SILAR	Successive ionic layer adsorption and reaction
SnSe	Tin Selenide
T	Transmittance
VB	Valence band
V_{oc}	Open circuit voltage
XPS	X-ray photoelectron spectroscopy
XRD	X-ray diffraction
ZnO	Zinc Oxide
ZnO:Al	Aluminium doped Zinc Oxide

ZnO:Sn	Tin doped Zinc Oxide
α	Absorption coefficient
η	Conversion efficiency
ρ	Sheet resistivity
σ	Electrical conductivity
Ω	Ohms

ABSTRACT

A solar cell is a device that converts light energy into electricity by photovoltaic effect. The photovoltaic effect refers to photons of light exciting electrons into a higher state of energy, allowing them to act as charge careers for an electric current. Materials presently used for solar cell fabrication include silicon, gallium arsenide (GaAs) among others. However, these materials are expensive and not readily available. As a result, there is need to search for alternative materials which are readily available and give a high conversion coefficient. The purpose of this research was to prepare and study the optical and electrical properties of Cu_xN_y and CdO:Al thin films so as to optimize them for solar cell applications. Cu_xN_y and CdO:Al thin films were deposited by dc magnetron sputtering and reactive evaporation techniques respectively using Edwards Auto 306 vacuum coater system. Cu_xN_y films were deposited at Nitrogen flow rates between 2 sccm and 10 sccm. CdO:Al films were deposited with Al doping concentrations of 0%, 1%, 3%, 5%, 7% and 9% atomic weight. The optical measurements were done using spectrophotometer Solid Spec 3700 DUV in the range (300-2000nm) while electrical characterization was done by four point probe method. Transmittance of Cu_xN_y films was found to increase with increase in wavelength and was below 20% in the 300-2000 nm range. For CdO:Al thin films, integrated transmittance was above 78% in the 400-800 nm range for all samples prepared. Reflectance of Cu_xN_y thin films was found to be below 30% in the 300-2000 nm range while that of CdO:Al thin films was below 15% in 400-800 nm range. From scout software, optical properties such as absorption coefficient, refractive index and extinction coefficient of the thin films were also obtained. For both Cu_xN_y and CdO:Al thin films, absorption coefficient decreased with increase in wavelength of incident radiation. Optical band gap of Cu_xN_y thin films increased with increase in Nitrogen flow rate to a maximum of 1.72 ± 0.02 eV at 10 sccm. For CdO:Al thin films, optical band gap increased with increase in Al doping to a maximum of 3.10 ± 0.06 eV at 5% Al doping, after which it started to decrease with increase in Al doping. Electrical resistivity of Cu_xN_y ranged from 31.70 Ωcm to 87.46 Ωcm while that of CdO:Al thin films ranged from 5.526×10^{-2} Ωcm to 11.33×10^{-2} Ωcm. Optimized deposition parameters such as nitrogen flow rate and Al doping concentration were used to fabricate a thin film solar cell on transparent glass slide. I-V characteristics of the solar cell were measured using a Keithley 2400 source meter interfaced with a computer running Labview program. An open circuit voltage of 476 mV, short circuit current density of 0.48 mA/cm^2, fill factor of 0.54 and conversion efficiency of 0.21 % were obtained. From these results, Cu_xN_y and CdO:Al thin films serve as potential alternative materials to the widely used silicon solar cells.

CHAPTER 1

INTRODUCTION

1.1 Background to the study

Photovoltaic effect is the direct conversion of solar energy to electricity. This source of energy forms one of the alternatives to large scale production of energy. Compared to other sources of energy, it is renewable, produces low greenhouse gases and uses no finite fossil fuel resources. Photovoltaics make use of solar cells which are fabricated from semiconductor materials. At present, materials used to fabricate solar cells are mainly silicon (Si), gallium arsenide (GaAs), cadmium-telluride (CdTe), and cadmium-indium-selenide (CIS). However, these materials are expensive and therefore this has become an issue (Jazairli, 2008). As a result, research for materials which are readily available and give a high conversion coefficient is on the rise. A solar cell uses solar energy that is inexhaustible, and is cheaply fabricated to produce power both for domestic and commercial purposes (Onyango, 2011). On comparison with other energy sources such as hydroelectric power and geothermal plants, it is relatively easy and cost effective to install and use the solar cells (Markvat, 1998). This power generation is environmental friendly as it produces minimal pollution. Furthermore, it is widely available and has no related transportation difficults.

In this research, Cu_xN_y and CdO:Al semiconductor thin films with optical characteristics such as direct energy band gap and high absorption co-efficient makes them more promising materials for application in photovoltaic cells. Copper Nitride (Cu_xN_y)

semiconductor thin film has a wide range of applications due to its high absorption co-efficient and suitability for optoelectronic applications (Lee *et al*., 2009). Its direct band gap energy lies between 1.2 eV and 1.9 eV and so can absorb light energy from the high energy end of the solar spectrum. It also has a superior optical transmission capable of improving conductivity and increasing current flow in a pn junction (Bindu *et al*., 2004).

CdO:Al is a transparent conducting oxide semiconductor suitable for application in photovoltaic cells. This is due to its low resistivity, high mobility wide band gap and low-cost of production (Wongcharoen *et al*., 2012). Cadmium, aluminium and oxygen are also readily available on the earth.

1.2 Statement of the research problem and justification

The use of major sources of energy such as fossil fuel has increased carbon dioxide emissions that cause global warming. In addition, these sources are not environment friendly due to pollution. As a result, there is need to develop alternative sources of clean energy. One such source is the solar energy which is utilized through photovoltaic process. Photovoltaic conversion is mainly done using silicon based solar cells. The process of obtaining industrial grade silicon is very expensive. To address this, there is an increasing interest in search for alternative materials for solar cell energy conversion with reduced cost of production. Although, much research has been done on Copper Nitride (Cu_xN_y) and Aluminum doped Cadmium oxide (CdO:Al) thin films, there is very little information on the combination of these materials to fabricate a solar cell. Hence, optical and electrical properties of these thin films making them suitable for solar cell applications were studied.

1.3 Objectives

1.3.1 Main objective

The main objective of this study was to prepare and characterize Copper Nitride (Cu_xN_y) and Aluminum doped Cadmium Oxide (CdO:Al) thin films for photovoltaic applications.

1.3.2 Specific objectives

(i) To prepare Cu_xN_y thin films by D.C magnetron sputtering.

(ii) To prepare CdO:Al thin films by reactive evaporation method .

(iii)To study electrical and optical properties of Cu_xN_y and CdO:Al thin films.

(iv)To fabricate and study I-V characteristics of Cu_xN_y-CdO:Al thin film solar cell.

1.4 Rationale

There is increasing demand for solar energy as an alternative source of energy because it is clean, renewable and abundant. To tap this source of energy, a converter is required. Solar cells have been fabricated from various semiconductor materials such as Silicon, Gallium, and Gallium Arsenide. However, the challenge has been the high cost of such materials and some of them are scarce. Thus, of interest is the search of new earth abundant materials capable of fabricating solar cells at low cost. Such materials include Copper and Nitrogen which are used to prepare Copper Nitride (Cu_xN_y) thin films. Copper nitride can be used as an absorber layer because of its narrow band gap and high absorption coefficient. Aluminum doped Cadmium oxide (CdO:Al) has shown desirable properties of a window layer such as wide band gap, high transmittance and low

reflectance. Hence this study will provide information on the combination of these materials to be used in solar cell.

In addressing environmental concerns on the use of cadmium, the amount of cadmium in CdO is very small and could be reduced even further as the cells become thinner. In contrast, coal burning and fertilizer production/use routinely generate Cadmium during operation. Therefore, cadmium used in solar cells pose little danger to the environment, which can be minimized by recycling the cells after their use.

CHAPTER 2

LITERATURE REVIEW

2.1 Introduction

This chapter reviews the history of thin film solar cells. It also presents related work done by various researchers in relation to preparation and properties of Copper Nitride and doped Cadmium Oxide thin films

2.2 Thin film solar cells

Photovoltaic phenomena were discovered in 1839 by a French physicist called Becquerel (Green, 2002). The first solar cell was fabricated by Charles Fritts in 1894, when he coated the semiconductor selenium with an extremely thin layer of gold to form the junctions (Nelson, 2003). The device was only around 1% efficient. Russell Ohl patented the modern junction semiconductor solar cell in 1946 which was 6% efficient (Chapin *et al.,* 1954). Many researchers have conducted research on various materials of thin films for solar cell applications. Among them includes $CuInSe_2/ZnO$, ZnO/In_2Se_3, $Cu(InGa)Se_2$, CuO/ZnO:Al and many more. These researches are basically aimed at improving the efficiency of solar cells, developing better fabrication technologies and coming up with new and better solar cell materials (Onyango, 2011).

2.3 Related literature on Copper nitride thin films

Gonzalez-Arrabal *et al*. (2010) deposited copper nitride thin films by dc triode sputtering from a commercial copper target onto a transmitting glass substrate. The study investigated the thermal stability of copper nitride (Cu_3N) thin films. For the as-deposited

films the calculated Nitrogen concentration was found to be 32 $\pm$ 2 at % corresponding to N-rich films. Optical characterization was done with a Woolman ellipsometer at room temperature and it revealed a direct transition of Cu_3N thin films.

Yue *et al*. (2005) prepared copper nitride (Cu_3N) thin films by reactive radio-frequency (RF) magnetron sputtering. It was found out that the deposition rate of the films gradually decreased with increasing nitrogen flow rate. The study revealed that films obtained by this method were strongly textured with crystal direction [100]. The Hall Effect measurements of the films revealed that the optical energy gap varied with the nitrogen content.

Fallberg (2010) reported the chemical vapour deposition of un-doped and oxygen doped copper (I) nitride. It was reported that oxygen doping increased the band gap of the material as well as electrical resistivity. XRD measurements showed that Cu_3N film deposited at high temperatures yielded grains with more well defined facets (111) than films deposited at lower temperatures.

Mikula *et al.* (2001) prepared copper nitride films by reactive dc sputtering onto glass and other substrates in nitrogen atmosphere. It was found out that the thickness, deposition rate, refractive index and optical band gap depended on the deposition pressure and power. The crystallographic nature of the films was investigated by X-ray diffraction. The films were further characterized by photoelectron spectroscopy (XPS), which confirmed that Cu_3N has a Nano-crystalline structure.

Xing-ao *et al.* (2011) studied copper nitride thin films prepared by reactive dc magnetron sputtering at various N_2-gas flow rates and different substrate temperature. It was found out that the N_2-gas flow rate and substrate temperature affect the deposition rate, the resistivity and the crystal structure of Cu_3N films. XRD measurements revealed that the films are composed of Cu_3N crystallites.

Copper nitride films deposited by Nosaka *et al*. (1999) by radio frequency sputtering presented a reddish dark brown colour. The deposition rate of the films gradually decreased and excessive nitrogen was added to the films as nitrogen partial pressure increased. The Copper Nitride films obtained by this deposition method were strongly textured with crystal direction [100]. The resistivity and the optical energy gap of the films were found to change with the nitrogen content.

Reddy *et al*. (2007) prepared copper nitride films on glass substrates by dc sputtering of copper target at a substrate temperature of 423 K under various nitrogen partial pressures. The dependence of cathode potential on the nitrogen partial pressure was explained in terms of nitridation of copper target and secondary electron emission. The effect of nitrogen partial pressure on the structural, mechanical, electrical and optical properties of copper nitride films was systematically investigated.

Yuan *et al*. (2006) reported that the electrical resistivity of copper nitride increases with increasing nitrogen content when measured at room temperature. Accordingly, the semiconductor nature of Cu_3N films can be understood by the non-stoichiometry of the films. For example, the low N_2 content in the sputtering process will result in more

copper doping in copper nitride and more free carriers. Hence the resistivity of the films decreases with decreasing the N_2 content.

Reddy and Uthanna (2007) deposited copper nitride on glass substrates using dc reactive magnetron sputtering technique under various sputtering powers. The thin films were characterized by studying the structural, electrical and optical properties. The effect of sputtering power on electrical resistivity and optical band gap were reported.

Pierson (2002) studied copper nitride thin films deposited by reactive RF magnetron sputtering of a copper target in various Ar-N_2 mixtures. The structure, hardness, electrical resistivity and optical band gap of these thin films were investigated. It was found out that at low nitrogen flow rate, the copper nitride films were sub stoichiometric whereas at high nitrogen flow rates, they were over stoichiometric in nitrogen. Electrical resistivity at room temperature and optical band gap of copper nitride films increased with the nitrogen flow rate.

2.4 Related literature on Cadmium Oxide and Doped Cadmium Oxide

Maity and Chattopadhyay (2006) prepared Aluminium doped cadmium oxide (CdO:Al) on a glass substrate by sol-gel dip-coating method. XRD pattern revealed the good crystallinity of CdO thin films. Optical study showed that the films had high transmittance. It was found out that the band gap depended on the content of Al in the films. Hall Effect measurements confirmed that the material is n-type. Mobility and carrier concentrations were also measured at various percentages of Aluminium.

Mahaboob *et al*. (2010) characterized CdO thin films prepared by Successive Ionic Layer Adsorption and Reaction (SILAR) deposition technique. The study determined the effect of molarity of solution on structural, optical and morphological properties of the deposited thin films. XRD and SEM revealed that the crystallite size of thin films increased with increase in molarity of the solution. UV-VIS spectrum of the films showed that the optical band gap energy increased with concentration of cadmium acetate in the precursor solution.

The structural, optical and electrical properties of boron-doped CdO thin films grown by vacuum evaporation on glass substrates have been investigated (Dakhel, 2011). It was found out that doped B^{3+} ions occupy locations in interstitial positions and/or Cd^{2+}-ions vacancies of CdO lattice. All the prepared B-doped CdO thin films showed degenerate semiconductors behavior. The conduction parameters were found to improve with boron doping.

Suhail *et al*. (2012) deposited Cadmium oxide thin films by thermal evaporation technique at different substrate temperatures on glass substrates. The XRD analysis showed that CdO films are amorphous and transform to polycrystalline with cubic structure when deposited at 448 K and annealed at 573 K. The direct band gap of CdO thin film decreased with increase of substrate temperature, while at an annealing temperature of 573 K the energy gap increased. Pure and doped-CdO films deposited by e-beam had a high optical transmittance in the visible region and polycrystalline structure (Mohamed *et al.,* 2006). Moreover, Xiu *et al.* (2006) studied CdO as a buffer layer to

improve the structural properties of ZnO films and using a thin buffer layer of CdO to enhance some physical properties of ITO film.

Highly transparent and conducting fluorine doped cadmium oxide (CdO:F) thin films were deposited on a glass slide by the sol-gel method (Santos-Cruz *et al*., 2007). The CdO:F thin films obtained showed high polycrystalline quality and high transmittance in the visible region. It was revealed that the band gap shift to higher energies was accompanied by a decrease in resistivity without a detrimental effect on transmittance, making the films good candidates for optoelectronic devices.

Ma *et al.* (2003) prepared CdO thin films on Si and glass substrates by dc magnetron sputtering method. The thin films grown on Si substrates had better crystallinity than that on glass substrates. The optical transmittance measurement showed that the thin films had a high average transmittance in the visible region and a direct band gap. By the electrical measurements, the thin films showed n-type conductivity.

Saha *et al.* (2007) studied electrical and optical properties of Al-doped cadmium oxide thin films deposited by RF magnetron sputtering. It was observed that optical band gap decreased first then increased with increase in Al doping. Further, electrical conductivity was found to increase with Al doping concentration before decreasing.

Transparent conducting aluminum doped cadmium oxide (CdO:Al) thin films have been deposited by spray pyrolysis method on glass substrates for various concentrations of aluminum (Kumaravel *et al.,* 2010). CdO:Al films were characterized using different techniques such as X-ray diffraction (XRD), atomic force microscopy, optical

transmittance and Hall measurement. XRD analysis showed that CdO films exhibit cubic crystal structure with (200) preferred orientation. The band gap values increased with doping and then decreased for higher Al doping concentration.

The influence of deposition temperature on structural, surface, optical and magnetic properties of the Al doped CdO thin films prepared by pulsed laser deposition (PLD) technique has been studied by Siraj *et al.* (2011). The optical constants (n, k, and optical band gap energy) of films measured by spectroscopic ellipsometry showed strong dependence upon deposition temperature.

Thin films of un-doped and Al-doped CdO have been prepared by thermal evaporation in vacuum on glass substrates (Wongcharoen *et al*., 2012). Energy gap, electrical conductivity, Hall mobility, electron concentration and temperature dependent resistivity were obtained. It was also found that the transition temperature is dependent on the Al concentration and is related to the increase in disorder induced by dopant addition.

2.5 Related thin film solar cells

A thin films solar cell consisting of n-type CdO and p-type NiO has been fabricated by home built spray pyrolysis technique (Inapasalini *et al*., 2012). Under illumination condition, the developed hetero-junction exhibited V_{oc} of 0.3 V, I_{sc} of 0.16 mA, a fill factor of 0.35 and conversion efficiency of 1.34 %. Yahiya (2008) made CdO/Si hetero-junction solar cell by vacuum evaporation of CdO thin film. I-V characterization of the cell under illumination was investigated; the cell showed an open circuit voltage (V_{oc}) of 0.4 V, a short circuit current density (J_{sc}) of 40 mA/cm^2, a fill factor (FF) of 0.34, and conversion efficiency (η) of 5.5%.

Omayio (2011) fabricated Cu_xO_y – ZnO:Sn pn junction solar cell by double deposition in steps using Edwards Auto 306 vacuum coater system. I-V characteristics of the solar cell were measured by Keithley 2400 source-meter interfaced with computer running LabView program. It had V_{oc} of 480 mV and fill factor of 0.63 which is higher than those of other cells in literature. The fabricated solar cell had conversion efficiency of 0.232%.

Tin doped cadmium oxide has also been used to fabricate SnSe-CdO:Sn pn junction (Makori, 2014). The diode characteristics obtained were; Isc = 0.993mA, I_{max} = 0.905mA, V_{oc} = 273mV, V_{max} = 207mV, FF = 0.69, and η = 0.59%

CHAPTER 3

THEORETICAL CONSIDERATIONS

3.1 Semiconductor materials and thin films

Conductivity of semiconductor materials lies between conductor and insulator materials. The conductivity of a semiconductor is generally sensitive to temperature, illumination, magnetic field and minute amount of impurity atoms (Abdullah, 2007). Semiconductors can be elemental semiconductors such as silicon (Si) or compound semiconductors such as CdSe in II-IV compounds. Furthermore, semiconductors can be grouped into direct band gap and indirect band gap semiconductors. In a direct semiconductor such as GaAs, an electron in the conduction band can fall to an empty state in the valance band, giving off the energy difference, E_g as a photon of light as shown in figure 3.1(a). On the other hand, an electron in the conduction band minimum of an indirect semiconductor such as Si cannot fall directly to the valance band maximum but must undergo a momentum change as well as changing its energy as shown in figure 3.1(b) (Al-Ayashi, 2007).

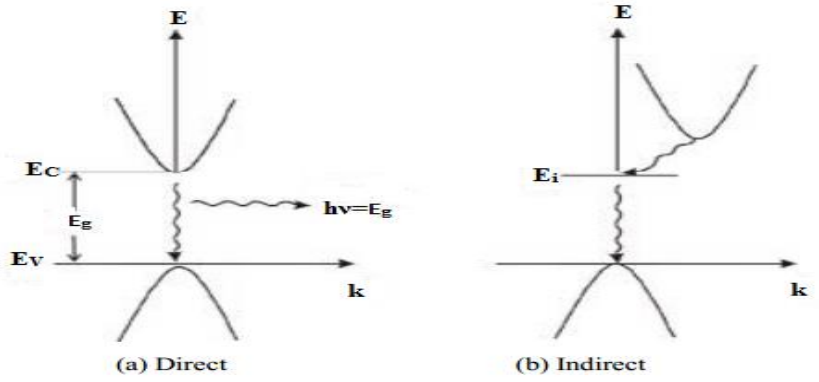

Figure 3.1: (a) Diagram illustrating direct electron transition (b) indirect electron transitions in semiconductors (Al-Ayashi, 2007)

For a semiconductor in which the minimum of the conduction band and the maximum of the valence band occur at the same value of k, absorption begins at $h\nu=E_g$ (hv is photon energy and E_g is the optical band gap) and the electron is transferred vertically between the two bands without a change in momentum. This transition is called direct allowed transition. For forbidden direct transition, the transition probability is increases with k^2.

Semiconductors are widely used in thin film technology and applications. A semiconductor material is said to be in thin film form only when it is built up as a thin layer on a solid support called substrate by a controlled condensation of the individual atomic, molecular, or ionic species (Orori, 2012). Thin films have unique properties which are different from their bulk counterparts. Hence they are used in optoelectronics, solar cells and smart windows among other applications.

3.2 Thin film preparation methods

3.2.1 Theory of evaporation method

Vacuum Evaporation is a thin film deposition technique performed by simply placing the material to be evaporated into a boat. The boat is normally made of materials which have very high melting point such as molybdenum (Mo). It then acts as a resistance element between two electrodes for the passage of large dc current. The substrate on which the film will be deposited is placed at a desired distance from the boat. The closer the substrate to the boat the faster a thin film will grow on the substrate. The material is

heated under vacuum until it melts and evaporates onto the substrate. Anything in the sight of the substrate will be coated with the evaporated material. The maximum evaporation rate is attained when the number of vapour molecules emitted corresponds to that required to exert the equilibrium pressure and this is governed by the Langmur Dushman kinectic theory given as, (Chopra, 1969);

$$\phi_e = \frac{3.513x10^{22} P_{e(torr)}}{\sqrt{MT}} \ , \tag{3.1}$$

where ϕ_e is the evaporation flux in number of atoms per unit area per unit time, P_e is the equilibrium pressure and M is the molecular mass evaporated at absolute temperature, T (in equilibrium). Evaporation relies on solid or molten sources which enter gas phase by physical mechanisms. The gaseous atoms are transported to the substrate surface in reduced pressure environment (Ohring, 1992). Deposition temperature is controlled by varying current to the heater.

3.2.2 Theory of sputtering method

Sputtering is the ejection of atoms from the surface of a material by means of the bombardment of surface with energetic particles. It consists basically of the bombardment of a target by emergent ions from a low pressure plasma causing erosion of material either atom- by – atom or as cluster of atoms and subsequent deposition of a film on a substrate (Cruz-Vazquez *et al*., 2001). The application of a high negative voltage to a target surface is the simplest way of inducing sputtering. This attracts positive ions

from plasma. This is the case for dc sputtering process used for targets that are composed of metals, or at least consisting of materials sufficiently electrically conducting that the target can act as an electrode. When the sputtering chamber containing the required gas, usually Argon (Ar), is maintained at a residual pressure of about 10^{-2} torr, a high voltage dc (1-3 kV) between cathode and anode, and a series of resistance of 1-10 kΩ, the charges are accelerated towards the cathode where they bombard the target material to eject the surface electrons. The ejected atoms traverse the medium and are deposited at the substrate on condensation.

3.3 Thin film Characterization Techniques

3.3.1 Optical characterization

3.3.1.1 Optical transmittance and reflectance

Optical transmittance and reflectance is measured by a Spectrophotometer. There are different models of this instrument such as UV-VIS-NIR spectrophotometer 3700 DUV, SHIMADZU-UV 3100 among others. These spectrophotometers work on the principle that when a beam of electromagnetic radiation of initial photon intensity, I_o, is incident on a transparent sample, photon intensity, I_t, is transmitted. Some part of the incident intensity could be absorbed while some part could be reflected. Transmittance and reflectance is read directly from the machine while absorbance is calculated from equation 3.2;

$$A + T + R = 1 \qquad (3.2)$$

The comparison between intensities of incident (I_o) and transmitted (I_t) photons is called transmittance and is given as;

$$\text{Transmitance (T)} = \frac{I_t}{I_o} \tag{3.3}$$

Reflectance is the percentage measure of the ratio of intensity of reflected light to that of incident intensity shone onto the surface of thin film. The two intensities are compared by measuring the intensity of the reference standard usually a highly reflecting material such as silver mirror at an incident angle of approximately 8 (Incident intensity) and that of the sample (reflected intensity) using a double beam spectrometer. The reflectance, R is given by;

$$\text{Reflectance (R)} = \frac{I_R}{I_o} \text{ X } 100\% \tag{3.4}$$

where I_R and I_o are intensities of the reflected and incident beams respectively.

3.3.1.2 Absorption of light

Absorption takes place when a photon with energy more than the band gap excites an electron from lower to higher energy state. Amount of absorption depends on photon wavelength, thickness of film and properties of the film. Intensity of photon transmitted (I_t) through the film of thickness, t, is given by;

$$I_t = I_o e^{-\alpha t} \tag{3.5}$$

where I_o is intensity of the incident photon and α is absorption coefficient. Rearranging equation 3.5, we get expression for α as;

$$\alpha = -\frac{(\ln T)}{t} \tag{3.6}$$

3.3.1.3 Optical band gap

The band gap (E_g) is the energy needed to move a valence electron into conduction band.

Absorption coefficient depends on the energy of light quanta according to Tauc's relation;

$$\alpha = \frac{(h\nu - E_g)^n}{h\nu} \tag{3.7}$$

where h is the Planck's constant (6.626 x 10^{-34} Js), ν is the frequency of the radiation and n gives the transition type which can either be direct or indirect. For direct band gap, $n = \frac{1}{2}$ (Mehta *et al*., 2009). Substituting for n in equation 3.7 and rearranging, gives;

$$(\alpha h\nu)^2 = h\nu - E_g \tag{3.8}$$

Thus, a plot of $(\alpha h\nu)^2$ against hν will give a curve with a straight line at certain portion. Extrapolation of the straight portion of the graph to the point of $(\alpha h\nu)^2 = 0$ gives the energy band gap, E_g.

3.3.1.4 Refractive index and extinction coefficient

Refractive index is related to dispersion and absorption of radiation by medium as (Serbetci *et al*., 2014);

$$\hat{n}\omega = n + ik \tag{3.9}$$

where n(ω) is the complex refractive index, n is the refractive index and k is extinction coefficient.

3.3.1.5 Scout software

OJL model has been employed to describe inter band transition in amorphous materials while drude model has been used to account for the movement of free electrons. OJL inter band model give expressions for the density of states for the optical transition from the valence band to conduction band. Parabolic bands are assumed with tail states exponentially decaying into the band gap as shown in figure 3.5 (O'Leary *et al.* 1997). The original parameters of OJL density of states model are energy, Ev and Ec, and the "damping constants" of the valence and conduction bands, γ_v and γ_c respectively. Included are the masses of the valence and conduction bands, m_v and m_c.

The expressions;

$$E_{m,v} = E_v - \frac{1}{2}\gamma_v \tag{3.10}$$

and;

$$E_{m,c} = E_c + \frac{1}{2}\gamma_c \tag{3.11}$$

denote the mobility edges of the valence and conduction bands respectively.

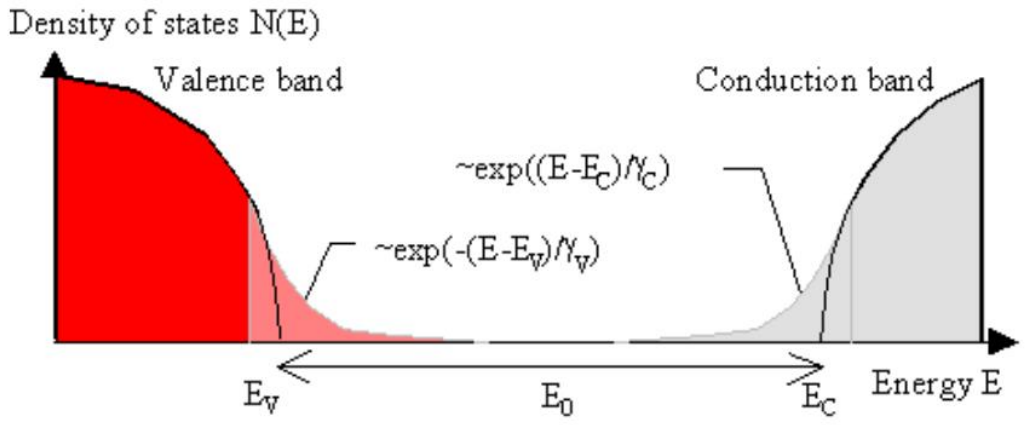

Figure 3.2: Diagram illustrating OJL model parameters (O'Leary, 1997)

The mobility gap, E_o, in the OJL is therefore given by;

$$E_0 = E_c + \frac{1}{2}\gamma_c - \left[E_v - \frac{1}{2}\gamma_v\right] \tag{3.12}$$

The band gap energy, E_g, is the difference between Ec and Ev values, i.e. the band gap in the case of no disorder, which is realized when both γ_v and γ_c, are zero

3.3.2 Electrical characterization

The sheet resistances of the thin films are measured using the four point probe method as shown in figure 3.6. In the four point probe method, measurements are made through four

contact terminals at each corner of the thin film labeled counterclockwise using Keithley 2400 Source meter.

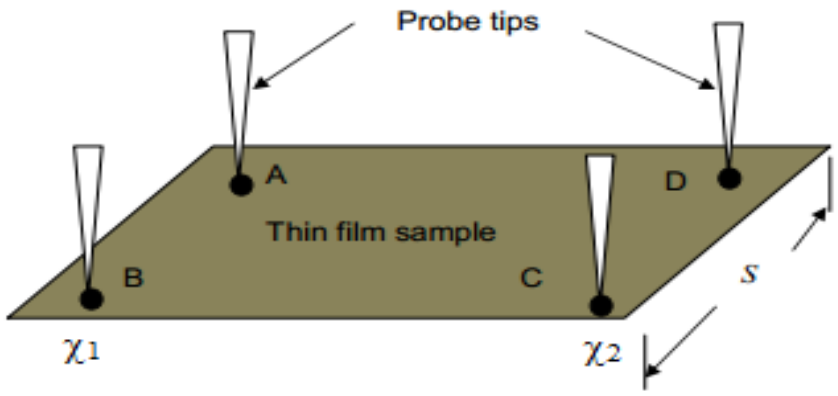

Figure 3.3: Schematic diagram of probe tips on sample film surface (Agumba, 2012)

Figure 3.3 shows a four point set up with a square geometry where current is sourced through side AB and voltage measured through side CD. Considering a very thin layer (thickness, t<< probe spacing, s), current rings instead of spheres are obtained (Brown and Jakeman, 1996). The differential sheet resistance, R_s is given by;

$$\Delta R_s = \rho\left(\frac{d\chi}{A}\right) \tag{3.13}$$

where, ρ is the sheet resistivity, A is the area of the film and dχ is a small change in distance along χ_1 χ_2 direction. Integrating equation 3.13, we obtain;

$$R_S = \int_{\chi_1}^{\chi_2} \rho \frac{d\chi}{A} \tag{3.14}$$

where ρ is resistivity.

Since the current area, A is given by;

$$A=2\pi\chi t \tag{3.15}$$

equation 3.14 becomes;

$$R_S = \int_{\chi_1}^{\chi_2} \rho \frac{d\chi}{2\pi\chi t} \tag{3.16}$$

From equation 3.16, equation 3.17 is obtained;

$$R_S = \int_{s}^{2s} \frac{\rho}{2\pi t}\frac{d\chi}{\chi} = \frac{\rho}{2\pi t}\ln 2 \tag{3.17}$$

Hence;

$$\text{Resistivity, } \rho = \frac{2\pi t R_S}{\ln 2} = 4.532 t R_s \tag{3.18}$$

The reciprocal of resistivity is called conductivity and is given by;

$$\text{Conductivity, } \sigma = \frac{1}{\rho} \tag{3.19}$$

3.4 Thin Film Solar Cell

3.4.1 Working Principle of a solar cell

The common configuration of a thin film solar cell is a p-n junction. A p-n junction is a layer formed from joining two parts, one p-type (holes being majority charge carriers)

and n-type (electrons are majority charge carriers) as shown in figure 3.7 (Soga, 2006). When a pn junction is formed, the large carrier concentration gradients cause the diffusion of carriers, that is, holes diffuse from p-type semiconductor to n-type semiconductor and electrons diffuse from n-type semiconductor to p-type semiconductor.

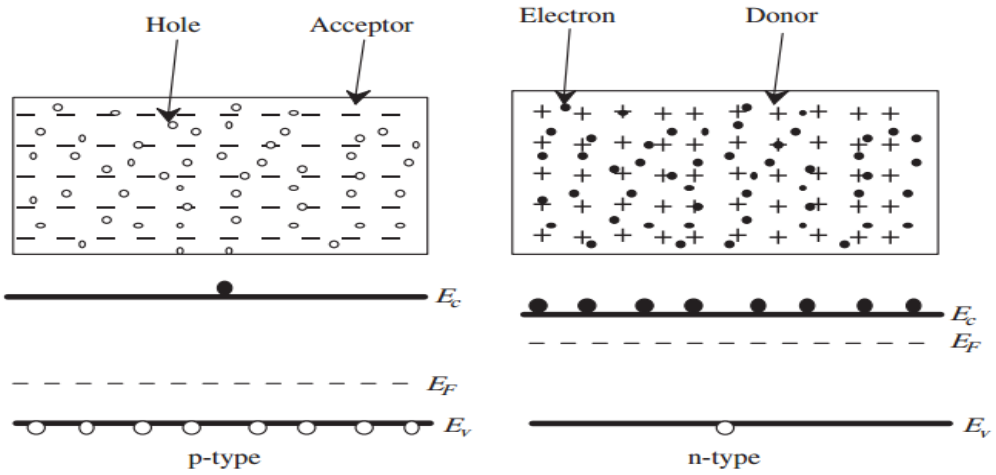

Figure 3.4: Energy band pictures and majority carriers of n- and p-type semiconductors (Soga, 2006)

Because of the ionized impurity atoms, a layer without mobile charge carriers is formed when the electrons and holes diffuse across the junction. This space charge sets up an electric field, which opposes the diffusion across the junction as shown in figure 3.5(a). When the drift current due to the electric field is balanced by the diffusion current because of the carrier concentration gradient for each carrier, the thermal equilibrium is established. At this point, the Fermi levels of the p-type semiconductor and n-type semiconductor are equal as shown in figure 3.5(b).

When the pn junction is irradiated, electron–hole pair is generated by the photons that have energy greater than the band gap. The number of electron–hole pair is proportional to the light intensity. Because of the electric field in the depletion region due to the ionized impurity atoms, the drift of electrons towards n-side and that of holes towards p-side occur in the depletion region. This charge separation results in the current flow from n- to p-side when an external wire is short-circuited as shown in figure 3.6.

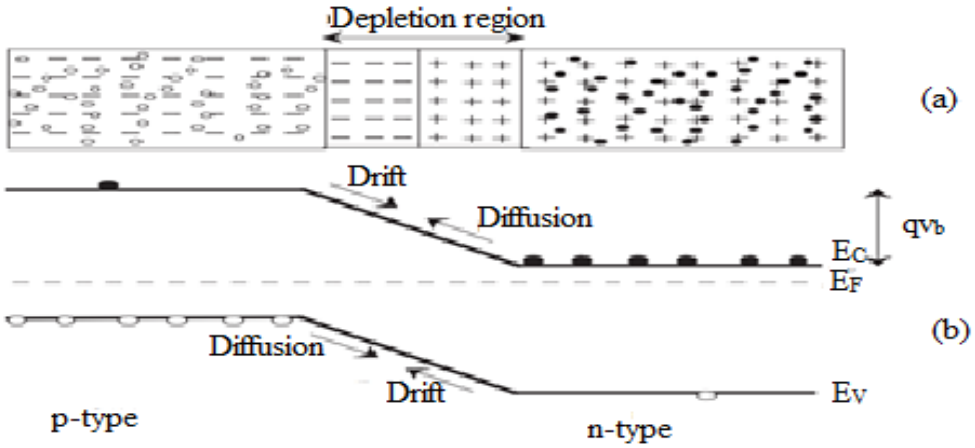

Figure 3.5: (a) Schematic diagram of pn junction (b) Fermi levels at thermal equilibrium (Soga, 2006)

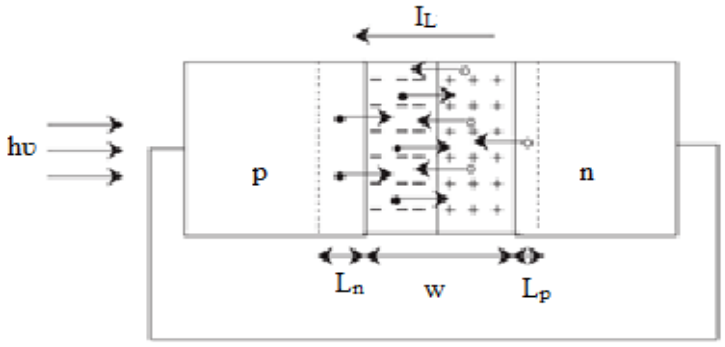

Figure 3.6: Schematic diagram of pn junction connected without a load

3.4.2 I-V Characterization

When the p- and n-side are connected without a load, the current is called the short-circuit current, I_{sc} and equals to the photogenerated current I_L. When the p- and the n-side are isolated, electrons move toward n-side and holes toward p-side, resulting in the generation of potential. The voltage developed is called the open-circuit voltage, Voc. Assuming that the area of the solar cell is unity, the current–voltage characteristic of the illuminated p–n junction is given by equation 3.20 (Soga, 2006);

$$J = J_o\left(\exp\left[\frac{qV}{kT}\right] - 1\right) - J_{SC} \tag{3.20}$$

where J is current density, J_o is dark saturation current density, V is voltage, k is Boltzmann's constant (8.62 x 10^{-3} eV/K), q is electron charge (1.60 x 10^{-19} C) and T is absolute temperature (373 K).

Under short circuit conditions, largest current is achieved. Short circuit current density (J_{sc}) is given by;

$$J_{sc} = J(V = 0) = J_L \tag{3.21}$$

Open circuit voltage V_{oc} (when J=0) is given by;

$$V_{oc} = \frac{AkT}{q}\ln\left[\frac{J_L}{Jo} + 1\right] \tag{3.22}$$

The above parameters that describe the working performance of a solar cell can be deduced from an I-V curve plotted under illumination. An example of such a curve is shown in figure 3.7.

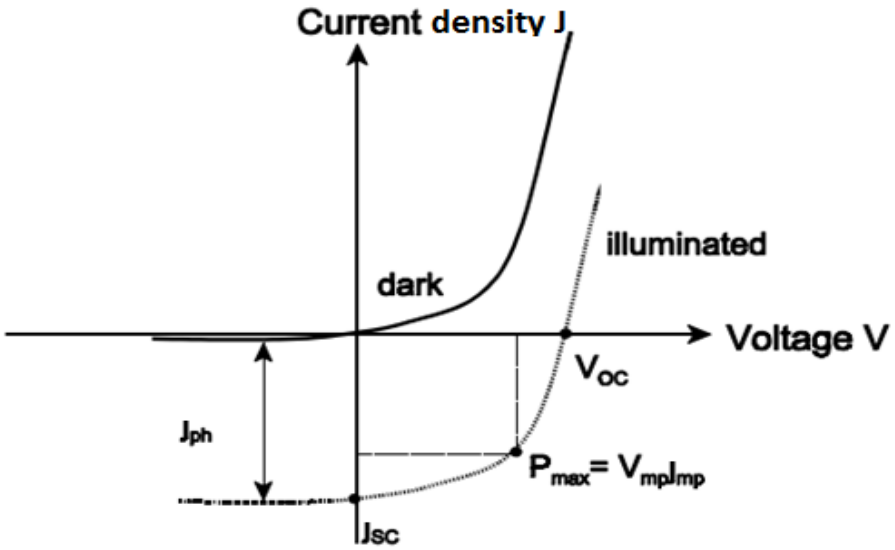

Figure 3.7: I-V characteristics of pn junction under illumination and darkness (Kemell, 2003)

From maximum power point, fill factor (FF) can be calculated. Fill factor measures quality of device through squareness of current and voltage curve and is given by;

$$FF = \frac{V_{max}J_{max}}{V_{oc}J_{sc}} \tag{3.23}$$

With total radiation (P_{in}) incident on thin film solar cell, conversion efficiency (ŋ) is given as;

$$\eta = \frac{V_{max}J_{max}}{P_{in}} \text{ x } 100\% \tag{3.24}$$

$$= \frac{V_{oc}J_{sc}\,FF}{P_{in}} \text{ x } 100\% \tag{3.25}$$

This value of conversion efficiency measures how good a solar cell is in photo conversion.

CHAPTER 4

EXPERIMENTAL PROCEDURES

4.1 Introduction

This chapter presents preparation and characterization of Cu_xN_y and CdO:Al thin films prepared by dc magnetron sputtering and reactive evaporation techniques respectively. The optical and electrical properties of the thin films were investigated using UV-VIS-NIR Solid Spec 3700 spectrophotometer and four point probe method respectively. The optimum deposition parameters were used to fabricate a thin film solar cell. A Keithley 2400 source meter interfaced with a computer running LabView was used to establish the device characteristics such as short circuit current density, open circuit voltage and the fill factor. The maximum current density, the maximum voltage and the power output of the cell were obtained from the I-V curve plotted. The details of the fabrication steps and characterization will be presented in the subsequent sections.

4.2 Thin film preparation

4.2.1 Cleaning of glass substrates

Microscope glass slides were used as substrate for thin film deposition. Before film deposition, they were cleaned with liquid detergent. They were then placed in pure alcohol to remove any grease and oil stains. They were then removed and thoroughly rinsed with distilled water. Thereafter, they were dried in an oven at 110^0c for about 30 minutes.

4.2.2 Preparation of Cu_xN_y thin films

Thin films of Cu_xN_y were deposited by dc sputtering method using Edwards Auto 306 sputtering machine. Figure 4.2 shows the schematic diagram of sputtering process. The cleaned glass slides were mounted to the rotating substrate holder. The copper target was then mounted on the magnetron and it was covered with a shutter about 4 cm above. The chamber was then closed and pumped down to 7.5 x 10^{-5} mbar. This was the best vacuum the machine could attain. Power was set at 140W and then argon and nitrogen gases were flown into the chamber separately at a flow rate of 20 sccm and 2 sccm respectively. Argon gas was used to effectively eject copper atoms from its surface. Pre-sputtering was done for 10 minutes to remove any oxides and impurities on the copper target. Copper vapour reacted with nitrogen forming copper nitride which was deposited as a thin film on the glass substrates.

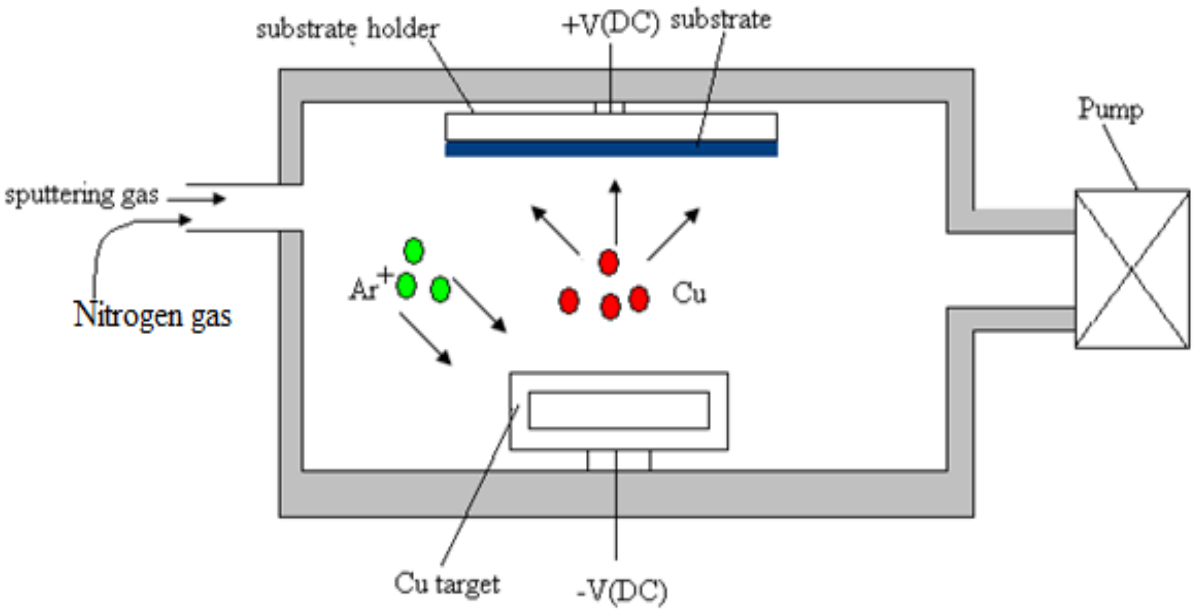

Figure 4.1: Schematic diagram of a sputtering system using copper target and oxygen gas.

Deposition time was 10 minutes. During sputtering, sputter pressure was maintained at 4.4 x 10^{-3} mbar. Similarly, other thin film samples were deposited at varying Nitrogen flows of 4, 6, 8 and 10 sccm. The prepared thin films were optically and electrically characterized for optimum deposition parameters.

4.2.3 Preparation of CdO:Al thin films

Thin films of CdO:Al were deposited by reactive evaporation method using Edwards Auto 306 coater. Cadmium was separately mixed with Aluminium at weight percentages 0%, 1%, 3%, 5%, 7% and 9% of Aluminium in a dry and clean glass tube. Each mixture was heated in closed glass tube until it melted to form Cd-Al compound. Figure 3.2 shows the diagram of the evaporation system. The cleaned microscope glass slides were mounted on the substrate holder. The compound of Cd and Al with 0% Al was placed in a molybdenum boat within the chamber.

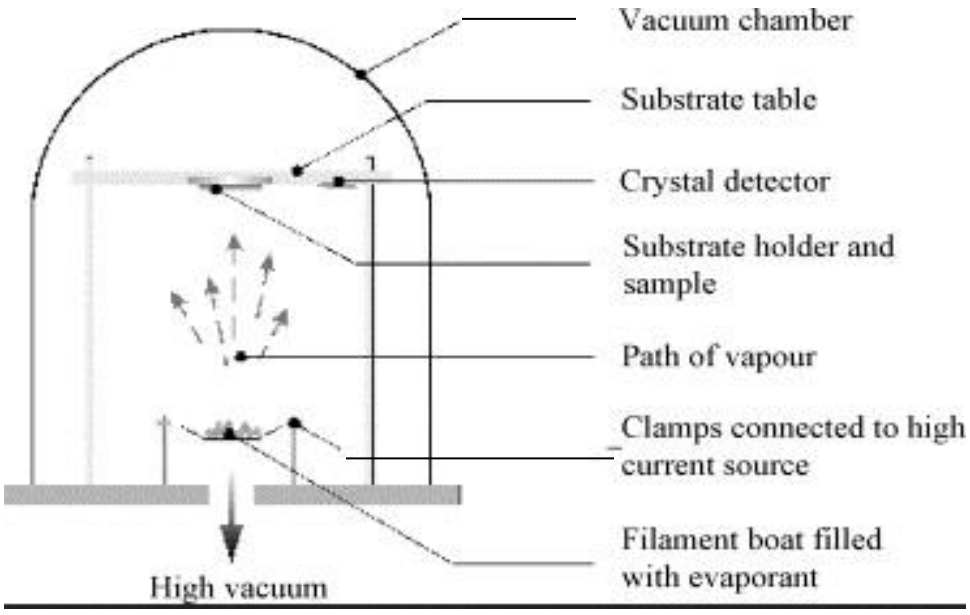

Figure 4.2: Schematic diagram of the evaporation system.

The chamber was then closed and pumped down to a pressure of 7.5×10^{-5} mbar. A current of 4.0 A was supplied to heat the Cd-Al compound. The shutter was removed to expose the Cd-Al vapour to the glass slide substrates in the presence of Oxygen flowing at 20 sccm. Aluminium-doped Cadmium Oxide (CdO:Al) was deposited on the glass substrate as a thin film. This procedure was repeated for the other Al compositions as well. The prepared thin films were optically and electrically characterized.

4.3 Optical characterization of the thin films.

Optical properties of Cu_xN_y and CdO:Al films were investigated separately. Transmittance and reflectance were measured using UV-VIS-NIR Spectrophotometer 3700 DUV that has a spectral range set between 300-2000 nm. Optical transmission measurements were obtained as shown in figure 4.3. Scout software by Wolfang Theiss (2012) was used to calculate optical parameters such as absorption coefficient, refractive index and extinction coefficient using transmittance and reflectance data. OJL and drude models were used.

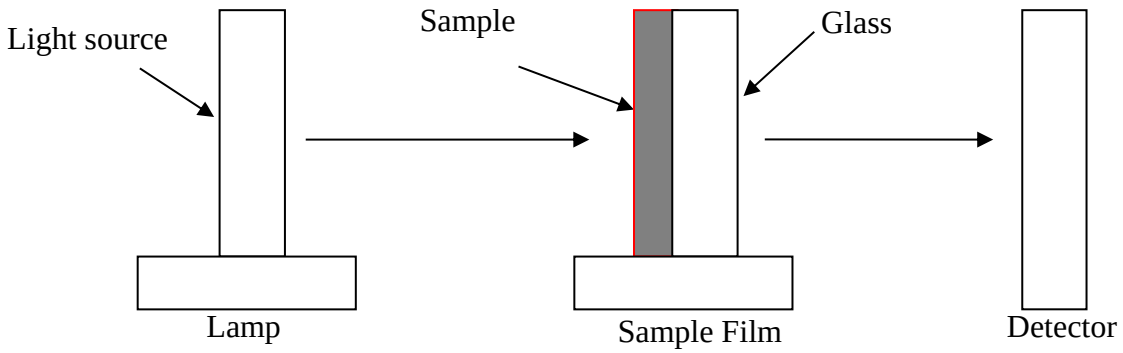

Figure 4.3: Schematic diagram for optical transmission measurement

4.4 Electrical characterization of the thin films

The sheet resistances of the thin films were measured by four point probe method using Keithley 2400 source meter. The electrical resistivity and conductivity were also calculated.

4.5 Cu_xN_y - CdO:Al thin film solar cell

4.5.1 Fabrication procedure

Using optimum deposition parameters, Ag/CdO:Al/Cu_xN_y/Ag solar cell device shown in figure 4.4 was fabricated in steps.

(i) Silver paste was pasted on a glass slide to form back contact electrode.

(ii) CdO:Al layer was then deposited by reactive evaporation.

(iii) Cu_xN_y was deposited on CdO:Al layer by dc magnetron sputtering.

(iv) Finally, Silver paste was pasted on Cu_xN_y layer to form front contact electrode.

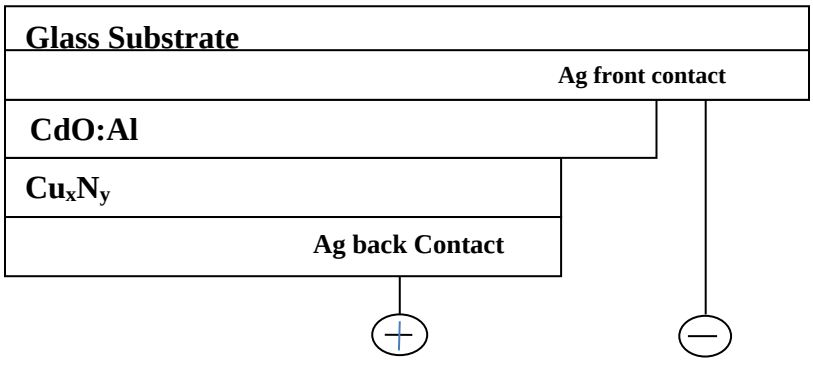

Figure 4.4: Schematic diagram for Cu_xN_y - CdO:Al solar cell.

4.5.2 I-V Characterization of the solar cell

Diode characteristics of the fabricated solar cell were determined from measurements of current density and voltage generated across the solar cell by use of Keithley 2400 sourcemeter interfaced with a computer running labview program. A current density against voltage (J-V) curve was plotted. Figure 4.2 is such a curve for a solar cell under illumination, showing how open circuit voltage (V_{oc}), short circuit current density (J_{sc}), maximum current density output (J_m), maximum voltage output (V_m) and maximum power point were determined. Fill factor, FF and conversion efficiency, η were calculated from equations 3.23 and 3.24 respectively.

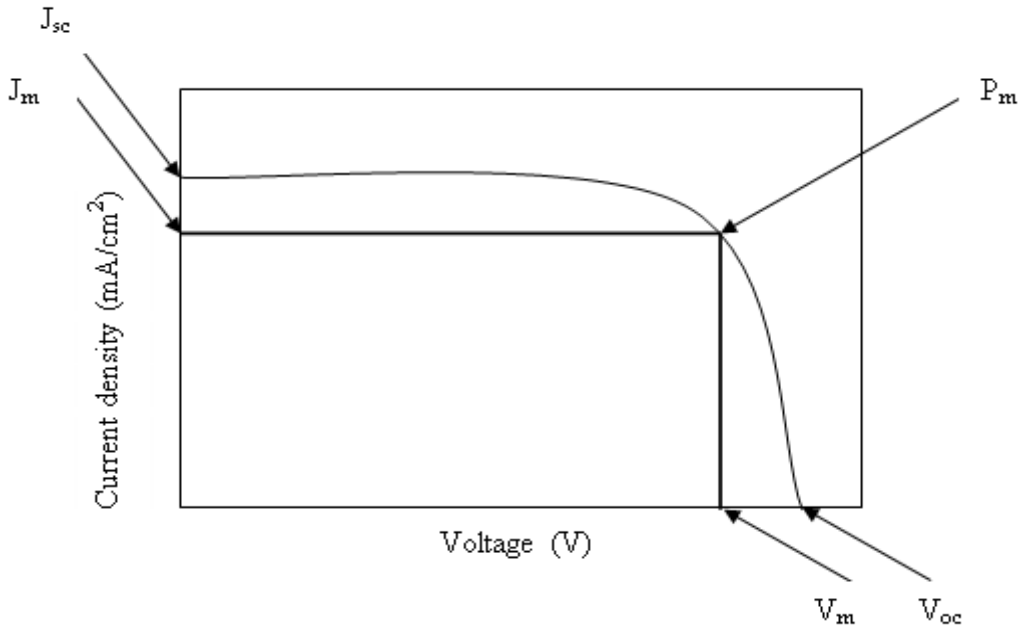

Figure 4.5: A graph showing I-V characteristics of an illuminated Solar cell (Pan, 2008)

CHAPTER 5

RESULTS AND DISCUSSION

5.1 Introduction

In this chapter, experimental results on the optical and electrical properties of Cu_xN_y and CdO:Al thin films are presented and discussed. The optical properties measured were transmittance and reflectance. The optical constants determined by Scout software such as absorption coefficient, band gap energy, refractive index and extinction coefficient are also discussed. Sheet resistance (R_s), electrical resistivity (ρ) and conductivity (σ) are the electrical properties studied. The chapter also includes results for J-V data of the fabricated solar cell.

5.2 Optical characterization of the thin films

5.2.1 Optical properties of Cu_xN_y thin films

5.2.1.1 Transmittance and Reflectance

Figure 5.1 shows the measured transmittance spectra of Cu_xN_y thin films. It was observed that transmittance was low over the visible range (400-800 nm) but higher over the near infrared region. This is because at lower wavelengths, the photon energy is higher than the band gap energy hence being absorbed. Average transmittance, T was obtained from equation 5.1 (Maghanga *et al*., 2011);

$$T = \frac{\int_{300}^{2000} T(\lambda)G(\lambda)d\lambda}{\int_{300}^{2000} G(\lambda)d\lambda} \qquad 5.1$$

where G(λ) is the air mass 1.5 spectrum. The values were presented as shown in table 5.1. It is observed that transmittance increased with increase in Nitrogen flow rate. The low transmittance in the case of films formed at low nitrogen flow rates was due to presence of copper phase along with copper nitride. The unreacted copper acts as scattering centres for light hence decrease in transmittance. At higher nitrogen flow rates higher transmittance was due to the decrease in scattering centres because of formation of single phase copper nitride thin films. Almost zero transmittance for the film deposited at Nitrogen flow rate of 2±0.2 sccm is a characteristic of copper thin films. All films had low reflectance as shown in figure 5.2.

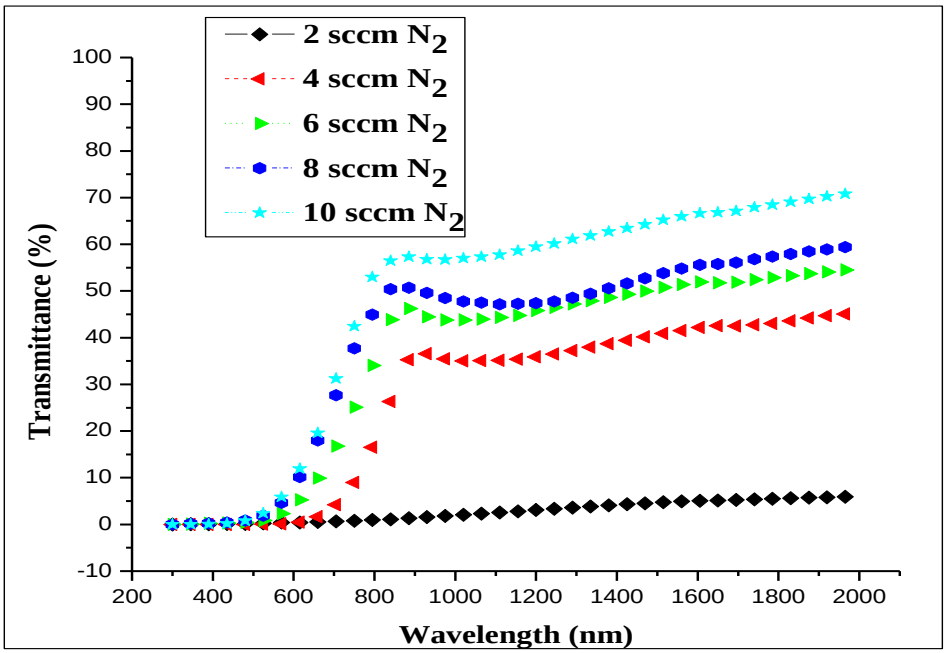

Figure 5.1: A plot of transmittance versus wavelength for Cu_xN_y films

Table 5.1: Average transmittance of Cu_xN_y films for different nitrogen flow rates.

N_2 Flow rate (sccm)	Average Transmittance (%) in 200-2000 nm range
2	0.77
4	9.12
6	13.26
8	15.63
10	18.46

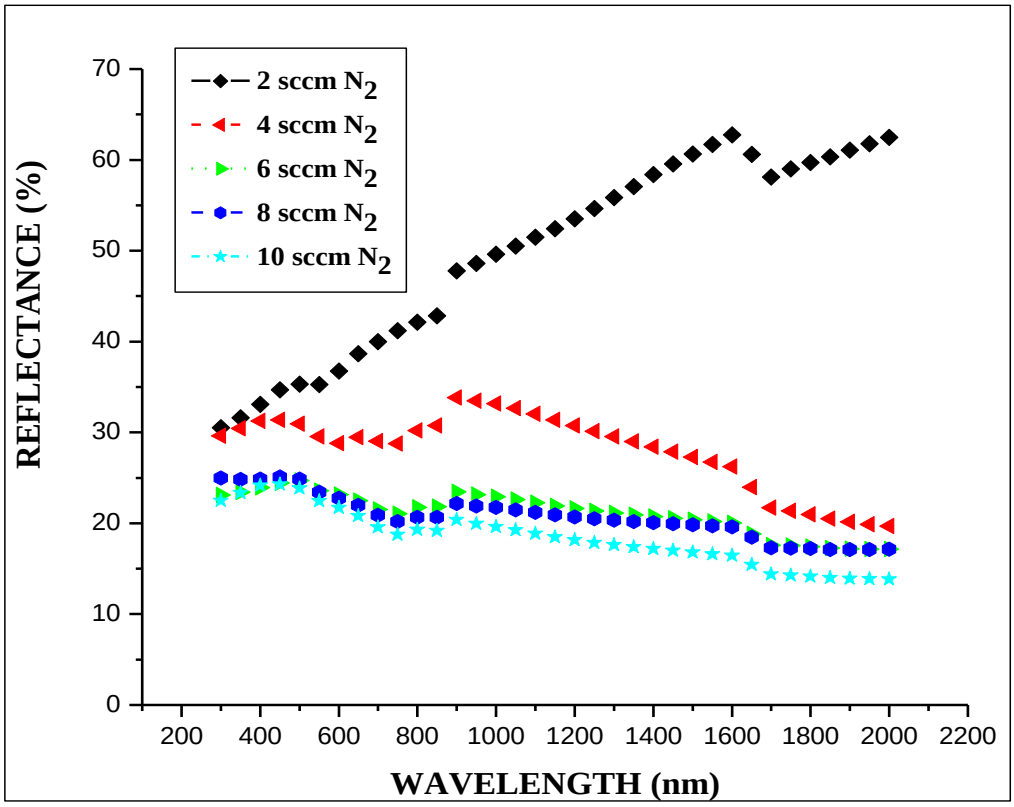

Figure 5.2: A plot of reflectance versus wavelength for Cu_xN_y films

5.2.1.2 Absorption coefficient of Cu_xN_y films

Fig 5.3 shows the plot of absorption coefficients of Cu_xN_y films. From this figure and table 5.1, it was observed that absorption of films decreases with increase in wavelength in the visible range. Absorption coefficient also decreases with increase in nitrogen flow rate in the 300nm – 2000 nm spectral range as shown in table 5.2. This can be attributed to decrease in copper atoms responsible for absorption as nitrogen content increases. This means the thin films becomes more stoichiometric as nitrogen content is increased. The fact that the calculated absorption coefficient, α values are at or above $10^5 cm^{-1}$ indicate that we are dealing with direct allowed optical transitions (Gordillo *et al*., 2008).

Table 5.2: Average absorption coefficient of Cu_xN_y films for different nitrogen flow rates.

N_2 flow rate (sccm)	Ave. α in 400 - 800 nm range x 10^5 cm^{-1}
4	2.86
6	2.17
8	1.82
10	1.68

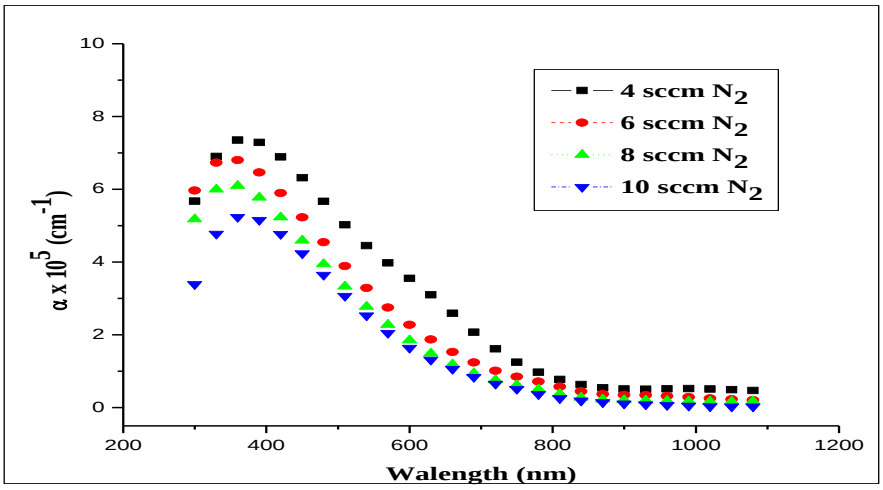

Figure 5.3: A graph of absorption coefficient versus wavelength for Cu_xN_y films

5.2.1.3 Band gap energy of Cu_xN_y films

The optical band gap was calculated from the relation between absorption coefficient, α, and photon energy, hν, given by equation 3.8. A plot of $(\alpha h\nu)^2$ against hν give a curve with a linear part. Extrapolation of the linear part to hν axis, the intercept gives the band gap energy. Figure 5.4 shows such a curve for the sample prepared with 4 sccm of N_2 gas flow rate. The band gap energy is found to be 1.54 ± 0.034 eV. The band gap energy for other N_2 flow rates is shown in table 5.3.

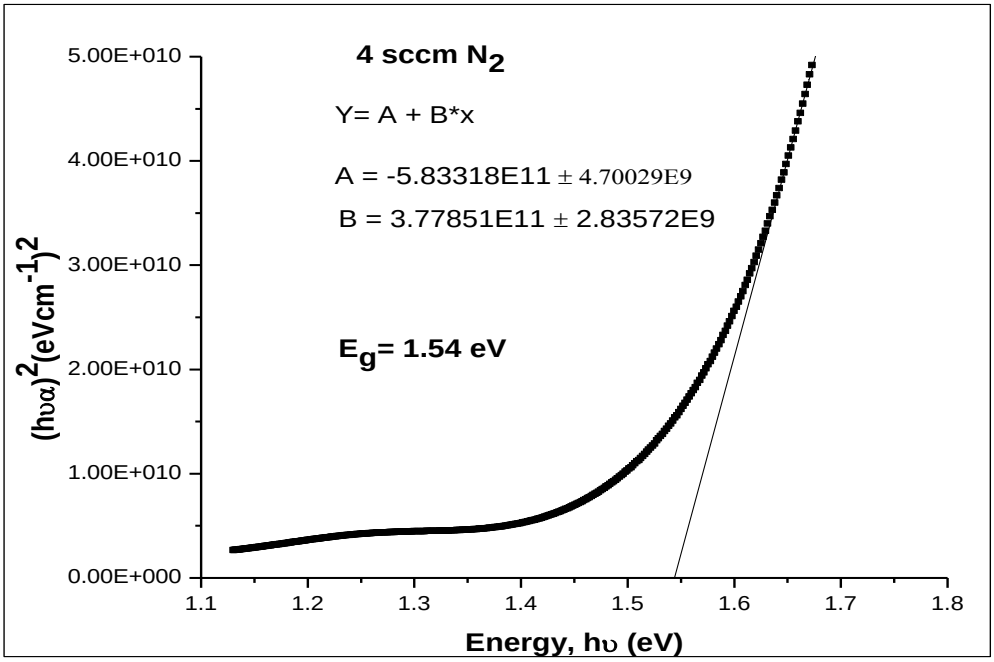

Figure 5.4: A plot of $(\alpha h\nu)^2$ against hν for Cu_xN_y films

The increase in band gap energy may be attributed to incorporation of Nitrogen atoms in the interstitial sites in the Cu-N structure and act as electron acceptor centres. The presence of a free-hole concentration at the top of the valence band should lower the fermi level and induce a corresponding increase in the energy of the lowest allowed

direct transition. The band gap energy at 2 sccm flow rate was not able to be calculated since the thin film formed was not of copper nitride but rather of copper thin film.

Table 5.3: Band gaps of Cu_xN_y films for different nitrogen flow rates.

N_2 Gas Flow Rate, ± 0.2 (sccm)	Band Gap Energy (eV)	Error
2	-	-
4	1.54	0.034
6	1.62	0.034
8	1.69	0.043
10	1.72	0.024

5.2.1.4 Refractive index of Cu_xN_y films

Figure 5.5 shows the spectral plot of refractive indices of Cu_xN_y films.

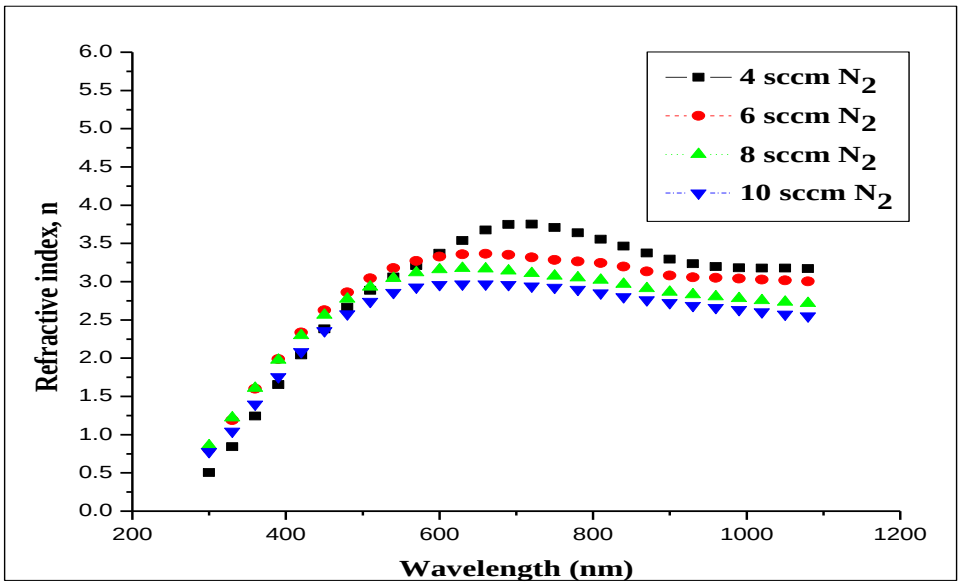

Figure 5.5: A graph of refractive index versus wavelength for Cu_xN_y films

For the sample deposited with 8 sccm of N_2 gas flow, it is observed that refractive index increases with increase in wavelength (below 600 nm) before remaining fairly constant. This may be attributed to strong absorption of Cu_xN_y and nitride thin films in this range (Dorranian *et al.*, 2012). This same trend is observed in all samples prepared. The obtained values for refractive indices are in good agreement with other reports (Reddy *et al.*, 2007; Dorranian *et al.*, 2009).

5.2.1.5 Extinction coefficient of Cu_xN_y films

Figure 5.6 show dependence of extinction coefficient on the wavelength and nitrogen flow rate. From the figure, it is seen that extinction coefficient decreases with increase in wavelength. It also decreases with increase in nitrogen flow rates. This may be attributed to reduction of defect centres which cause absorption and thereby decrease extinction coefficient values.

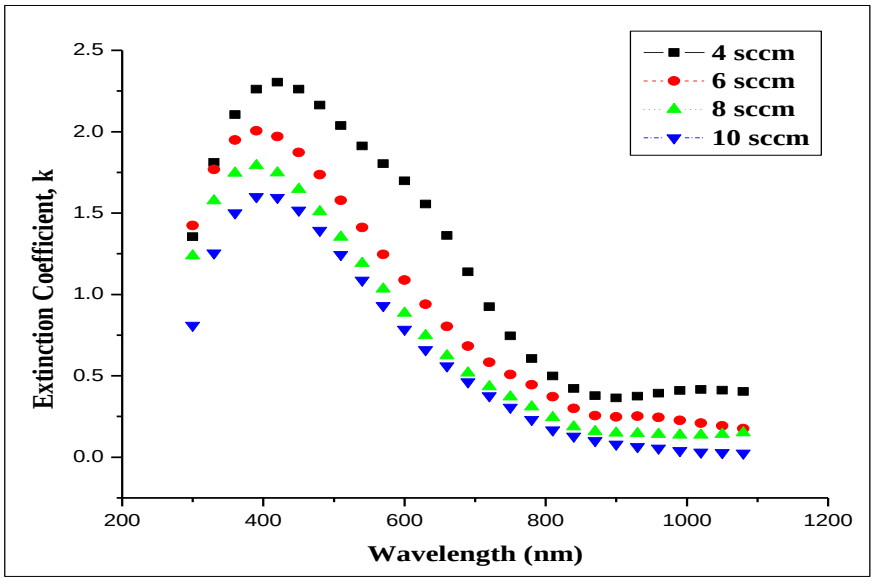

Figure 5.6: A plot of extinction coefficient versus wavelength for Cu_xN_y films

5.2.2 Optical properties of CdO:Al thin films

5.2.2.1 Transmittance and Reflectance

The transmittance spectrum in figure 5.7(a) shows that the thin films have high light transmission in the visible range. The integrated transmittance of undoped CdO was found to be 78% while that of doped CdO thin films ranged from 79.01% to 85.91 % in the $400 \leq \lambda \leq 800$ nm range. It is also observed that average transmittance increased with Al doping percentage up to 5% then decreases as seen from table 5.6. Generally, Al doping enhanced transmittance of the undoped CdO thin films. However, when Al doping percentage increased beyond 5%, transmittance decreased. This decrease may be attributed to disorder in the lattice due to excess Al dopant. High transmittance of CdO:Al thin films in the visible range shows that it is a good material for use in photovoltaic applications.

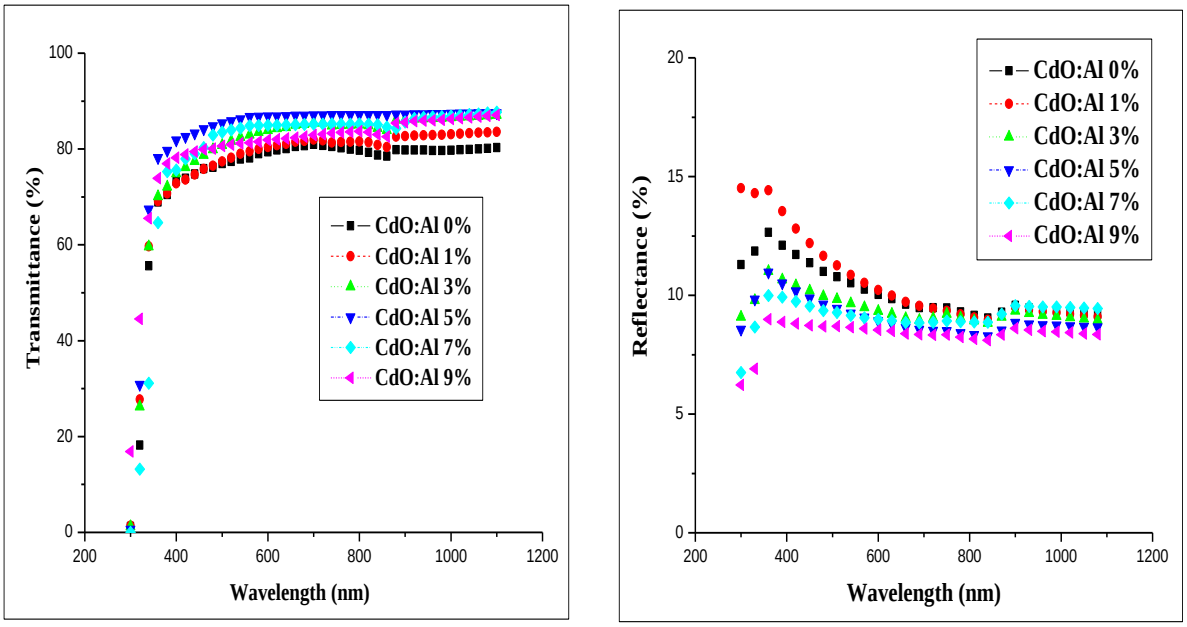

Figure 5.7: Transmittance spectra (a) and Reflectance spectra (b) for CdO:Al films

From figure 5.7(b), reflectance of CdO and CdO:Al thin films ranged from 6 to 14% in in the $400 \leq \lambda \leq 800$ nm range. Generally, Aluminium doped CdO thin films had lower reflectance than the undoped CdO thin films. This low reflectance implies the thin films have high transmittance in the visible range and this makes them suitable to use as window layer in solar cell applications.

Table 5.4: Average transmittance of CdO:Al films for different Al doping %.

Al doping %	Average Transmittance (%) in 400-800 nm range
0	78.26
1	79.01
3	82.32
5	85.91
7	83.47
9	81.41

5.2.2.2Absorption coefficient of CdO:Al films

The spectral plot of absorption coefficient of CdO:Al thin films is shown in figure 5.8. It is observed that absorption coefficients decrease with increasing wavelength. At high wavelengths, absorption is low which indicates that the films are optically transparent to photons incident on their surface. However at small wavelengths absorption coefficients are high since absorption of incident photon takes place. The decrease in absorption coefficient with increase of wavelength within the visible spectrum energy range (400 –

800nm) indicated that the films are transparent at low energies. This is because at low energies, band gap energy is not exceeded hence electrons are not excited from top of valence band to conduction band.

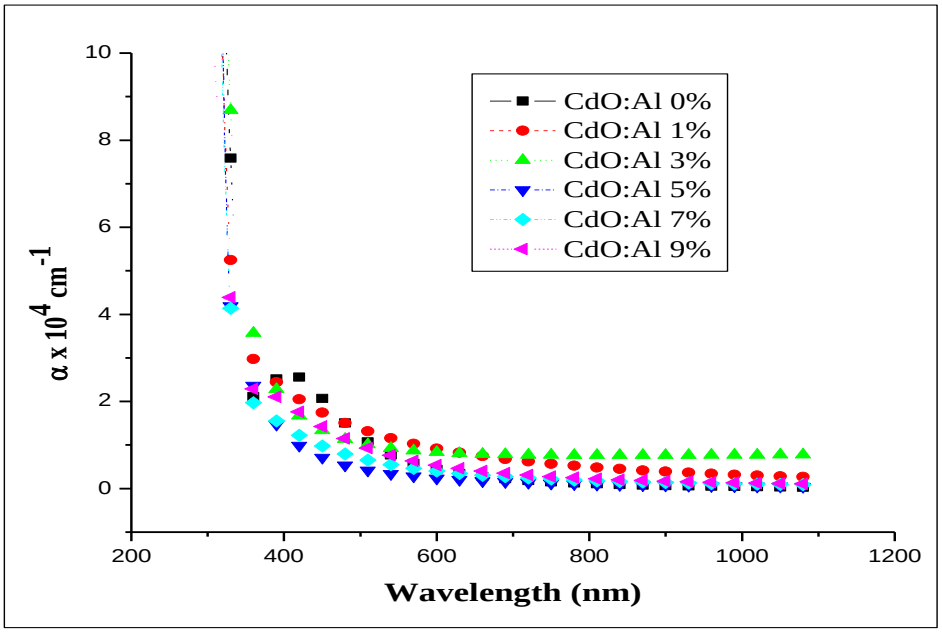

Figure 5.8: A plot of absorption coefficient versus wavelength for CdO:Al films

Generally, it is noted that Al doping has insignificant effect on absorption coefficient. This is also observed from the transmittance spectra of CdO thin films .

5.2.2.3 Band gap energy of CdO:Al thin films

Absorption coefficient is related to photon energy according to equation 3.8. Figure 5.9 shows a plot of $(\alpha h\nu)^2$ against hv for the sample prepared with 5% Al doping. The point on hv axis where $(\alpha h\nu)^2 = 0$, gives the value of the band gap as 3.10 ± 0.062 eV for this sample. Other values of the band gap are shown in table 5.5.

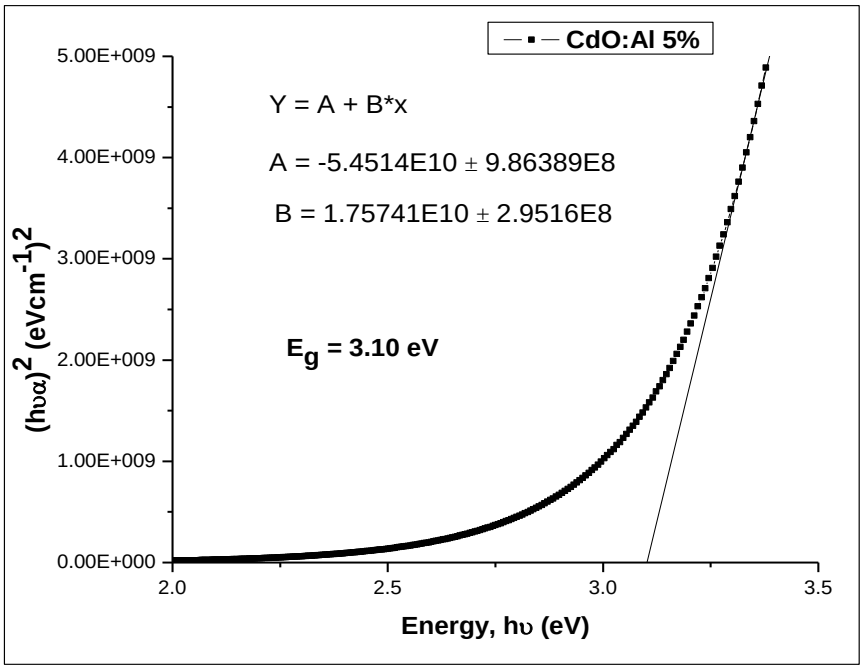

Figure 5.9: A graph showing curve of $(\alpha h\nu)^2$ against $h\nu$ for CdO:Al films

Table 5.5: Band gaps of CdO:Al films for different Al doping %

Al doping %	Band Gap Energy (eV)	Error
0	2.51	0.050
1	2.63	0.052
3	2.84	0.057
5	3.10	0.062
7	2.96	0.059
9	2.80	0.056

From figure 5.10, it is observed that as the Al doping percentage is increased, the band gap energy increases up to an optimum value of 3.10 eV at 5% doping. Further doping

results in a decrease in band gap. The increase in band gap energy with increase in Al doping may be attributed to Burstein-Moss effect (Kumaravel *et al.*, 2010). This effect occurs when the carrier concentration exceeds conduction band edge density of states, which corresponds to degenerate doping in semiconductors. As the doping concentration increases, more and more donor states are produced which pushes Fermi level higher in energy, resulting to increase in band gap.

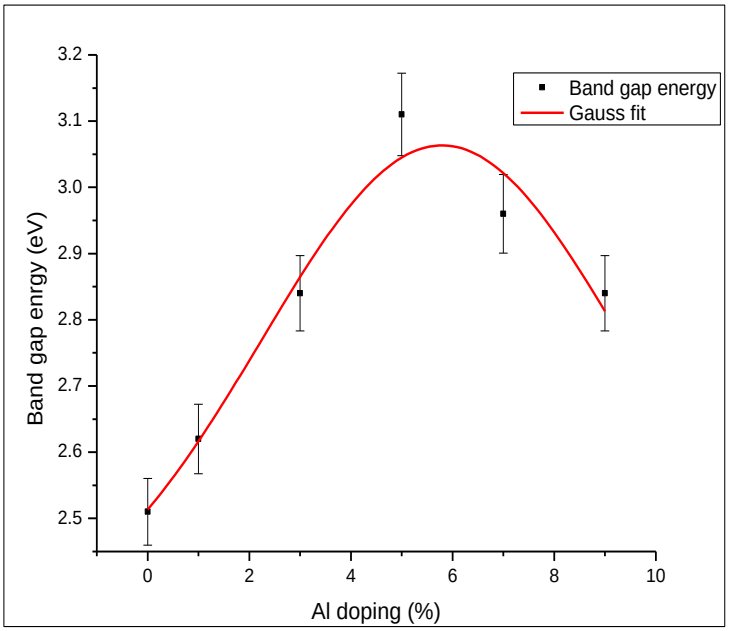

Model	Gaussian		
Equation	$y = y_0 + Ae^{-\frac{(x-x_c)^2}{2w^2}}$		
		Value	Error (±)
	Y_o	2.36	0.22
	X_c	5.66	0.24
	w	3.29	0.99
	A	0.70	0.21

Figure 5.10: A graph showing Variation of band gap energy with al doping percentage

5.2.2.4 Refractive index of CdO:Al thin films

As shown in figure 5.11, there is no significant change in refractive indices with increase in wavelength from 400 nm to 800 nm. However, refractive index decreased with increase in Al doping before increasing again at 5 % Al doping. Un-doped CdO thin film had a refractive index of 1.63, which decreased to 1.43 at 5% Al doping.

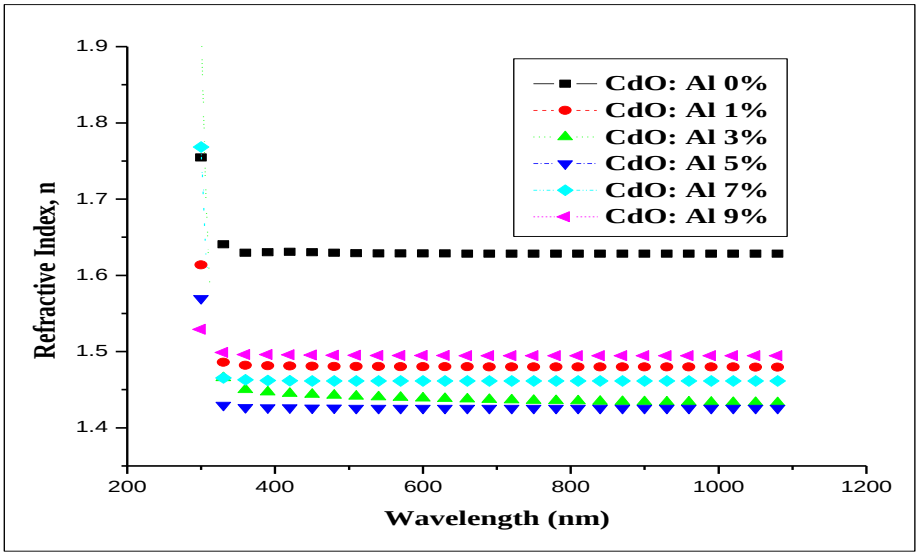

Figure 5.11: A graph of Refractive index versus wavelength for CdO:Al films

5.2.2.5 Extinction coefficient of CdO:Al thin films

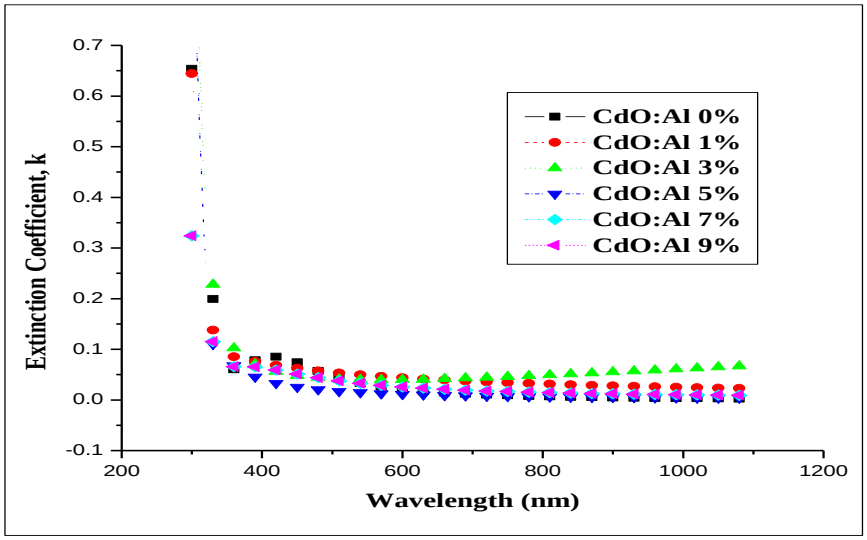

Figure 5.12: A graph of extinction coefficient versus wavelength for CdO:Al

The figure 5.12 shows a plot of how extinction coefficient varies with wavelength. All the films showed low extinction coefficient, showing that the films had low photon

energy absorption loses and this is a requirement for a good window layer (Makori *et al*., 2014). It is also observed that there is a slight dependence of extinction coefficient on doping concentration, having the lowest value at 5 % Al doping.

5.3 Electrical Characterization of the thin films

5.3.1 Electrical properties of Cu_xN_y thin films

5.3.1.1 Electrical Resistivity

Sheet resistance measurements were done by four point probe using Keithley 2400 source meter. The obtained values are used to calculate resistivity using equation 3.16 and given in table 5.6. Figure 5.13 shows the variation of electrical resistivity with Nitrogen flow rate. Resistivity increases with increase in Nitrogen flow rate, to a maximum value of 87.46 ± 0.44 Ωcm at Nitrogen flow rate of 8.0 sccm. The low electrical resistivity at lower nitrogen flow rate may be attributed to the presence of mixed phase of copper along with the copper nitride.

Table 5.6: Electrical resistivity of Cu_xN_y films for different nitrogen flow rates.

N_2 Flow rate ±0.2 (sccm)	Resistivity, $\rho x10^1$ (±0.005) Ωcm
4	3.17
6	7.77
8	8.75
10	8.45

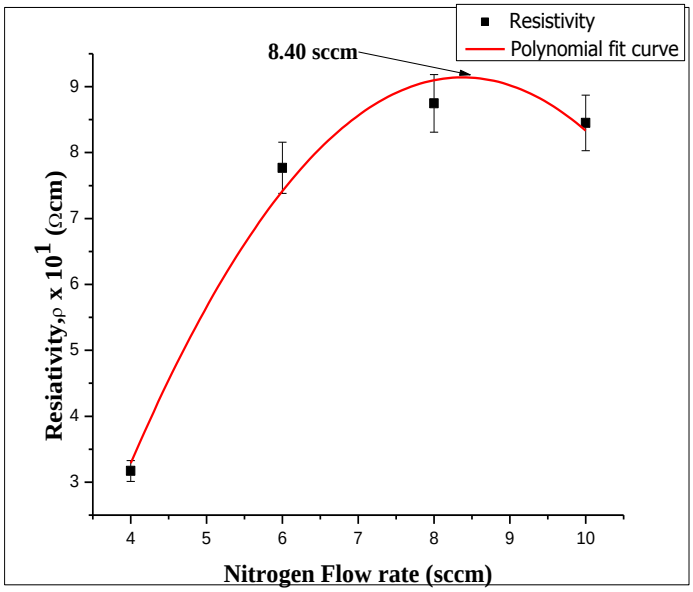

$Y = Intercept + B1x\text{^}1 + B2x\text{^}2$

	Value	Error (±)
Intercept	-12.31	3.02
B1	5.12	0.93
B2	-0.31	0.07

Figure 5.13: A graph showing variation of resistivity with nitrogen flow rate

5.3.1.2 Electrical Conductivity

The conductivity was evaluated from equation 3.17 and results tabulated as shown in table 5.7. As expected, conduction decreases with increase in N_2 flow rate to a minimum of 1.14 x 10^{-2} $(\Omega cm)^{-1}$ at N_2 flow rate of 8.0 sccm

Table 5.7: Electrical conductivity of Cu_xN_y films for different nitrogen flow rates.

N_2 Flow rate (±0.2) sccm	Resistivity, ρx10^1 (±0.005) Ωcm	Conductivity, σ x 10^{-2} (±0.005)$(\Omega cm)^{-1}$
4	3.17	3.15
6	7.77	1.29
8	8.75	1.14
10	8.45	1.18

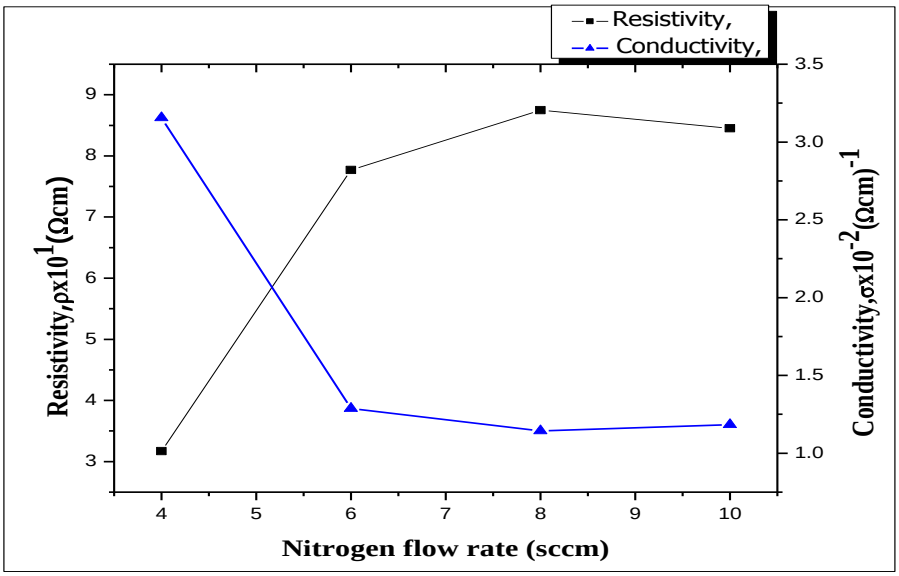

Figure 5.14: A plot showing variation of resistivity and conductivity with nitrogen flow rate

5.3.2 Electrical properties of CdO:Al thin films

5.3.2.1 Electrical Resistivity

Figure 5.15 shows the variation of resistivity with Al doping percentage. From table 5.8, it is observed that resistivity decreases with increase in Al doping percentage to a lowest value of 5.53 X 10^{-2} Ωcm at 5% Al doping. Decrease in resistivity may be attributed to increase in free charge carriers due to substitution of cadmium atoms by aluminium atoms. The substitution of Cd^{2+} with Al^{3+} results to an extra free charge carrier leading to increased charge carriers. However, beyond 5.45% Al doping, the extra Al atoms occupy the interstitial positions and form Al_2O_3 leading to distortion of the crystal structure which gives rise to higher resistivity.

Table 5.8: Electrical resistivity of CdO:Al films for different Al doping %.

Al doping (%)	Resistivity, $\rho x10^{-2}$ (±0.005) Ωcm
0	11.33
1	9.01
3	6.93
5	5.53
7	6.03
9	7.96

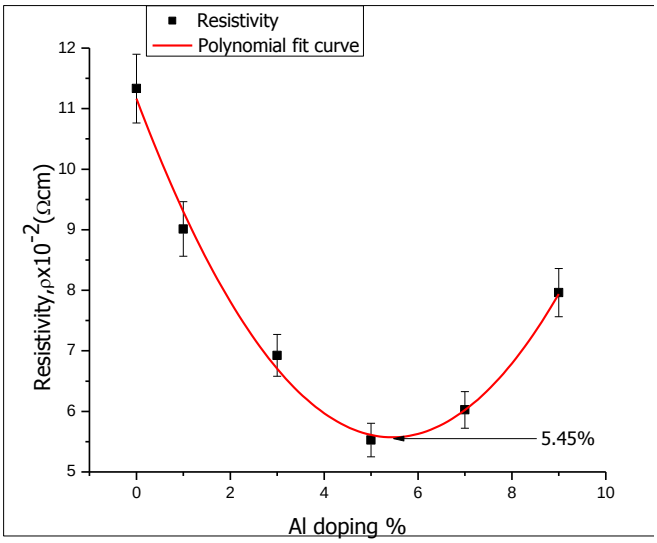

$Y = Intercept + B1x\text{^}1 + B2x\text{^}2$

	Value	Error (±)
Intercept	11.16	0.24
B1	-2.05	0.11
B2	0.19	0.01

Figure 5.15: A graph showing variation of resistivity with Al doping %

5.3.2.2 Electrical Conductivity

Table 5.9 shows electrical conductivity as evaluated from equation 3.19. Figure 5.16 shows the variation of electrical conductivity with Al doping percentage.

Table 5.9: Conductivity of CdO:Al films for different Al doping %.

Al doping (%)	Resistivity, $\rho x10^{-2}$ (±0.005) Ωcm	Conductivity ,$\sigma x10^{1}$ (±0.0005) $(\Omega cm)^{-1}$
0	11.33	0.88
1	9.01	1.11
3	6.93	1.44
5	5.53	1.81
7	6.03	1.66
9	7.96	1.26

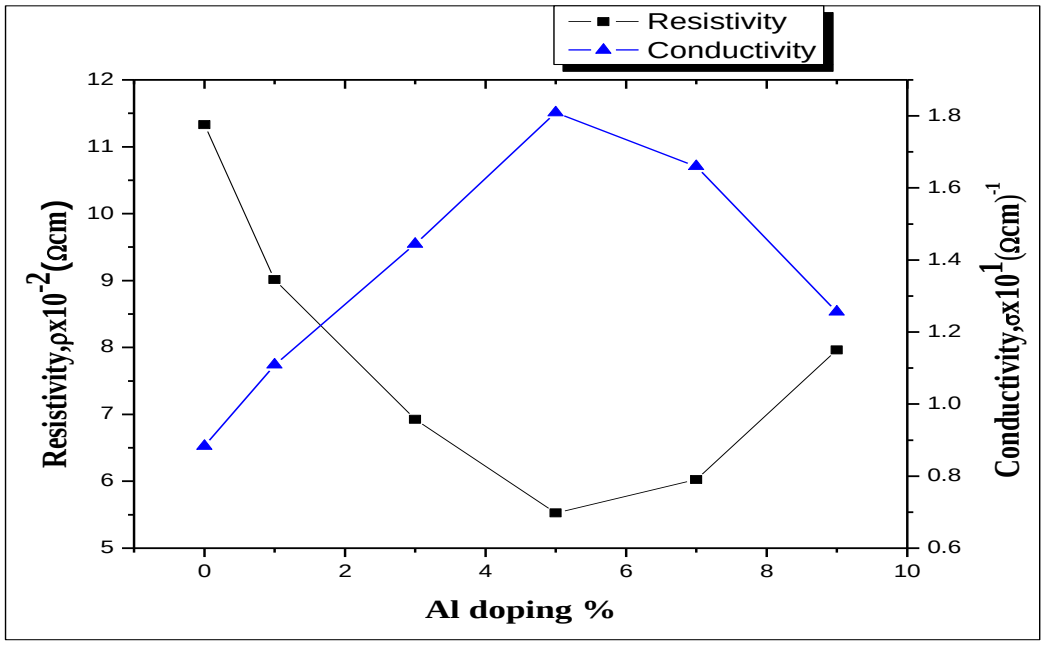

Figure 5.16: A plot showing variation of resistivity and conductivity with Al doping %

5.4 Optimized deposition Parameters

Nitrogen flow rate of 8.0 ±0.2 sccm was chosen to fabricate Cu_xN_y absorber layer. From the optimized electrical resistivity, this sample showed that the prepared films were stoichiometric. The sample also had a narrow band gap of 1.69 ± 0.043 eV, high absorption coefficient and low transmittance in the visible range. For CdO:Al, 5% Al doping was chosen to deposit a window layer for a thin film solar cell fabrication. This is because the film showed highest average transmittance of 85.91 % in the visible range, highest band gap energy of 3.10 ± 0.062 eV and lowest resistivity of 5.53×10^{-2} Ωcm.

5.5 I-V characteristics of Cu_xN_y-CdO:Al solar cell

Table 5.10 shows a plot of J-V characteristics as shown in figure 5.7 of the fabricated thin film solar cell. From the figure, diode parameters such as short circuit current density (J_{sc}), open circuit voltage (V_{oc}), current density at maximum power output (J_m), and voltage at maximum power output (V_m) were determined. Fill factor (FF), and conversion efficiency (η) were calculated using relationships shown in equation 3.23 and equation 3.24 respectively.

The fabricated photovoltaic cell had a short circuit current density, J_{sc} = 0.480 mA/cm^2, open circuit voltage, V_{oc} = 476 mV, a fill factor, FF = 0.54 and energy conversion efficiency, η = 0.21 %. It can be observed that the value of short circuit current density is generally low. This is due to electron-hole recombination and high resistance of the front

and back silver contacts of the solar cell. It can also be seen from the square-like nature of the curve in figure 5.7 and a fill factor of above 0.50 that the pn junction formed was of good quality. The conversion efficiency obtained is higher than that of other solar cells reported by Kidowaki *et al*. (2012) and comparable to that obtained by Makori *et al.* (2014).

Table 5.10: Voltage, Current density and power density of the solar cell

Voltage, V (V)	Current density, J (mA/cm^2)	Power density (W/cm^2)x 10^{-5}
0.476	0	0
0.456	0.071	3.24
0.406	0.185	7.51
0.356	0.299	10.64
0.306	0.402	12.30
0.256	0.437	11.19
0.206	0.455	9.37
0.156	0.468	7.30
0.106	0.478	5.07
0.056	0.479	2.68
0	0.480	0

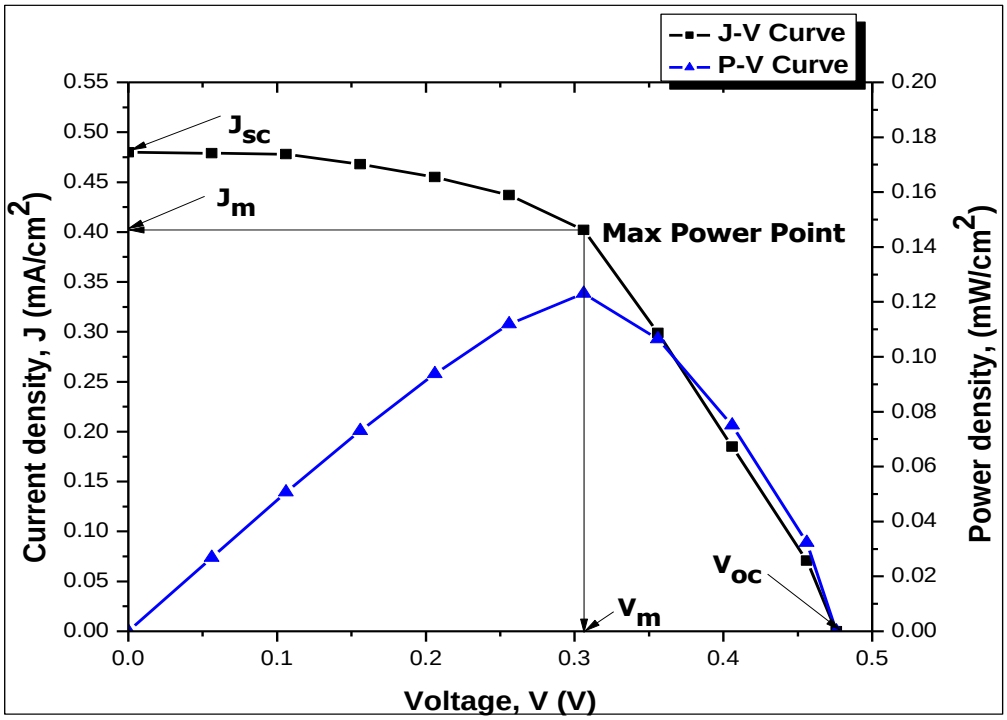

Figure 5.17: A graph showing how current density and power density varies with voltage curves

CHAPTER 6

CONCLUSIONS AND RECOMMENDATIONS

6.1 Conclusions

Thin films of Cu_xN_y and CdO:Al have been successfully prepared by direct current sputtering and reactive evaporation techniques respectively. The Edwards Auto 306 vacuum coater machine was used for all the film depositions. Both optical and electrical properties of the films deposited were investigated. The transmittance and reflectance of the thin films were measured using Solid spectrophotometer DUV 3700 over the range 300-2000 nm. Four point probe interfaced with Keithley-2400 source meter was used for sheet resistivity measurement which was used to calculate the resistivity of the thin films. For Cu_xN_y thin films, transmittance increased with increase of Nitrogen flow rate. Reflectance was generally low, below 20% within the visible range. As Nitrogen flow rate increased, band gap energy was observed to increase from 1.54 eV at 4 sccm N_2 flow rate to 1.72 eV at 10 sccm N_2 flow rate. Absorption coefficient was of order 10^5 cm^{-1} within the visible range for all deposited thin films. Resistivity increased with increase in N_2 flow rate from 31.7 Ωcm at 4 sccm to an optimum value of 87.46 Ωcm at 8 sccm of N_2 flow.

The transmittance measurements showed that Al doping enhanced transmittance of CdO thin films. The optimum integrated transmittance of 85.91 % was obtained at 5% Al doping. Reflectance of less than 20% was obtained for all thin films in the UV-VIS range. Doping had an effect of increasing the optical band gap of CdO films from 2.51

eV of un-doped CdO to a maximum of 3.10 eV for Al doping concentration of 5%. This is attributed to more free carriers present due to Al doping. The refractive index reduced with increase in Al doping percentage to a minimum at 5 %. For electrical properties of CdO:Al thin films, resistivity varied between 1.33 X 10^{-1} Ωcm and 5.53 X 10^{-2} Ωcm as Aluminium doping increased from 0 % to 5 % Al doping. This was due to the substitution of Al^{3+}at the Cd^{2+}sites that created extra free carrier that decreased resistivity to an optimum value at 5% Al doping. Increase in resistivity after 5% doping may be attributed extra Al atoms occupying the interstitial positions and formation of Al_2O_3 leading to distortion of the crystal structure.

From the optimized deposition parameters, glass/CdO:Al/Cu_xN_y/Ag solar cell was successfully fabricated. It had a short circuit current density, J_{sc}, of 0.48 mA/cm^2, open circuit voltage, V_{oc}, of 476 mV, a fill factor, FF, of 0.54 and energy conversion efficiency, η, of 0.21 %. From these results, Cu_xN_y and CdO:Al thin films have been put forward as potential alternative materials to the widely used silicon solar cells.

6.2 Recommendations

For further research, there is need to study the effect of annealing on the optical and electrical properties of Cu_xN_y and CdO:Al thin films. Secondly, more deposition parameters should be studied to find out how they affect the optical and electrical properties of these thin films. Such parameters include deposition power, temperature, film thickness, various substrates, nitrogen partial pressure and substrate temperature for

Cu_xN_y thin films. For CdO:Al, effect of film thickness should be studied for the optimum Aluminium dopant. Thirdly, chemical analysis should be done to find out the content of copper and nitrogen in Cu_xN_y thin film. Fourthly, it is recommended that a study be done on structural properties of these thin films using X-Ray diffraction (XRD). Again, the use of a different back and contact in the pn junction such as gold is highly recommended. This can possibly make a better ohmic contact and hence improve the open circuit current of the solar cell. In addition, it is recommended that anti-reflective coating (ARC) be applied on the surface of CdO:Al window layer to reduce the amount of light reflected hence increase the photon energy absorbed. Lastly, it is recommended that I-V characterization be done with a high light intensity on a small area solar cell so as to improve its conversion efficiency.

REFERENCES

Abdullah, S., (2005). Preparation and characterization of chlorine doped cadmium sulphide thin films and their applications in solar cells. M.Sc thesis, Kings University, Saudi Arabia.

Agumba, J. O. (2010). Design and fabrication of a simple four point probe system for electrical characterization of thin films. Thesis, Department of Physics. Kenyatta University.

Al-Ayashi, W.M., (2007). Influence of annealing on the optical & electrical properties of chlorine doped CdS thin films and their Applications. Msc. Thesis. King Saud University, Saudi Arabia.

Bindu, K. and Nair, P. (2004). Semiconducting tin selenide thin films prepared by heating Se-Sn. *Journal of Science and Technology*, **19**:1348-1353.

Brown, M. and Jakeman, F., (1996). Theory of four point probe technique as applied to film layers on conducting substrates. *British Journal of Applied Physics*, **17**: 1146-1149.

Chopra, K. L**.,** (1969). Thin film phenomenon. McGraw-Hill Book Company, New York. Pg 96, 477.

Chapin, D.M., Fuller, C.S. and Pearson, G.L., (1954). A new Silicon p-n Junction Photocell for converting solar Radiation into electrical Power. *Journal of Applied Physics*, **25**: 676-677.

Cruz-Vazquez, A., Rocha-Alonzo, F., Burrel-Ibarra, S.E., Inoue, M. and Bernal, R., (2001). Fabrication and characterization of sulphur doped zinc oxide thin films. *Superficies Y Vacio*, **13**: 89-91.

Dakhel, A.A., (2011). Structural, optical and electrical measurements on boron-doped CdO thin films. *Journal of Material Science*, **46**: 6925-6931.

Dorranian, D., Dejam, L., and Mosayebian, G. (2012). Optical characterization of Cu_3N thin film with swanepoel method. *Journal of Theoretical and Applied Physics*, **6**:1-9.

Dorranian, D., Dejam, L., Sari, A.H. and Hojabri, A., (2009). Effect of nitrogen content on optical constants of copper nitride thin films prepared by DC magnetron reactive sputtering. *Journal of Theoretical and Applied Physics*, **3**(3): 37- 41.

Fallberg, A., (2010). Chemical vapor deposition of undoped and oxygen doped copper (I) nitride:Digital comprehensive summaries of Uppsala Dissertations from the Faculty of Science and Technology. *Acta Universitatis Upsaliensis*, **691**:1-52.

Gonzalez-Arrabal, R., Gordillo, N., Martin-Gonzalez, M.S., Ruiz-Bustos, R. and Agullo-Lopez, F., (2010). Thermal stability of copper nitride thin films: The role of Nitrogen migration. *Journal of Applied Physics*, **103513**:1-7.

Gordillo, N., Gonzalez-Arrabal, R., Martin-Gonzalez, M.S., Olivares, J., Revera, A., Briones, F., Agullo-Lopez, F. and Boerma, D.O., (2008). DC triode sputtering deposition and characterization of N-rich copper nitride thin films: Role of chemical composition. *Journal of Crystal Growth*, **310**:4362–4367.

Green, M.A., (2002). Photovoltaic principles. Physica E, **14**:11-17

Inpasalini, M.S., Gayathri Davi, R., Balamurugan, D., Jeyaprakash, B.G. and Rayappan, J.B., (2012). Spray deposited thin films metal oxide based heterojunction for solar cell application. *Journal of Applied Sciences*, **12**(16):1742-1745.

Jazairli, M.A., (2008). Growth of zinc oxide nanoparticles on top of polymers and organic small molecules as a transparent cathode in tandem photovoltaic device. M.Sc thesis, Department of Science and Technology, Linkoping University, Sweden.

Kemell, M., (2003). Electrodeposition of $CuInSe_2$ and doped ZnO thin films for solar cells. Academic dissertation, May 2003. Department of Chemistry, University of Helsinki.

Kidowaki, H., Oku, T. and Akiyama, T., (2012). Fabrication and Evaluation of CuO/ZnO Heterostructures For Photoelectric Conversion. *International Journal for Research and Reviews in Applied Science*, **13** (1):67-72.

Kumaravel, R., Meneka, S., Snega, S.R., Ramamurthi, K. and Jeganathan, K., (2010). Electrical, optical and structural properties of aluminum doped cadmium oxide thin films prepared by spray pyrolysis technique. *Materials Chemistry and Physics*, **122**: 444–448.

Lee, Y.S., Bertoni, M., Chan, M.K., Ceder, G. and Buonassisi, T., (2009). Earth abundant materials for higher efficiency heterojunction thin film solar cells. Photovoltaic Specialists Conference (PVSC), 34th IEEE. 002375-002377.

Ma, D., Ye, Z., Wang, L., Hung, J. and Zhao, B., (2003). Deposition and characteristics of CdO films with absolutely (200)- prepared orientation. *Material Letters*, **58**: 128-131.

Maghanga, C.M., Niklasson, G.A., Granqvist, C.G. and Mwamburi, M., (2011). Spectrally selective surfaces for heat reduction in concentrator solar cells: Modelling and applications of TiO_2:Nb-based thin films. *Applied Optics*, **50**(19):3296-3302.

Mahaboob, B., Anusuya, M. and Saravanan, V., (2010). Characterization of CdO thin films prepared by SILAR deposition technique. *International Journal of Chemical Engineering and Applications*,**1**: 151-154.

Maity, R. and Chattopadhyay, K.K., (2006).Deposition of CdO:Al on glass substrate by sol-gel dip-coating method.*Journal of Science*, **20**(4): 97-102.

Makori, N.E., Amatalo, I.A., Karimi, P.M. and Njoroge, W.K., (2014). Optical and Electrical properties of CdO:Sn thin films for solar cell applications. *International Journal of Optoelectronic Engineering*, **4**(1):11-15.

Markvart, T., (1998). Solar Electricity.John Wiley & Sons publishers, New York. 3-4, 34-35.

Mehta, S.K., Kumar, S., Chaudhary, S. and Bhasin, K.K., (2009). Nucleation and growth of surfactant passivated CdS and HgS NPS: Time dependent absorption and luminescence profiles. *Supplimentary Materials (ESI) for Nanoscale*, 1-6.

Mikula, m., Buc, D. and Pincik, E., (2001). Electrical and optical properties of copper nitride thin films prepared by reactive DC magnetron sputtering. *Acta Physica Slovaca*, **51**:35-43.

Mohamed, H.A., Ali, H.M., Mohamed, S.H. and Abd El-Raheem, M.M., (2006). Transparent Conducting ZnO-CdO thin films deposited by e-beam evaporation technique. *Journal of Applied Physics*, **34**:7-12.

Nelson, J., (2003). The Physics of Solar Cells. Imperial College Press, London. 2-8.

Nosaka, T., Yoshitake, M., Okamoto, A., Ogawa, S. and Nakayama, Y., (1999). Copper nitride thin films prepared by reactive radio-frequency magnetron sputtering. *Thin Solid Films*, **348**:8-13.

Ohring M., (1992). The material science of thin films. Academic Press Ltd, London, 79-84,109.

Omayio, E.O., (2011). Characterization of Cu_xO_y – ZnO:Sn P-N Junction For Solar Cell Applications. M. Sc. thesis, Department of Physics, Kenyatta University, Kenya.

Onyango, M.C., (2011). Characterization of Sn_xSe_y-zno:Al P-N junction for solar cell applications. M. Sc. thesis, Department of Physics, Kenyatta University, Kenya.

Orori, M.C., (2012). Electrical and Optical Characterization of $Cd_xZn_{1-x}S$ and PbS thin Films For Photovoltaic Applications. M. Sc. thesis, Department of Physics, Kenyatta University, Kenya.

O'Leary, S., Johnson, S. and Lim, P., (1997). The relationship between distribution of electron states and the optical absorption of an amorphous semiconductor. *Journal of Applied Physics*, **82**:3334.

Pan, J., (2008). Material Property Study on Dye Sensitized Solar Cells and Cu (Ga,In)Se_2 Solar Cells. M. Sc. Thesis, Department of Paper and Chemical Engineering, Miami University, Oxford.

Pierson, J.F. (2002). Structure and properties of copper nitride films formed by reactive magnetron sputtering. *Journal of Vacuum Technology*, **66**:59-64.

Reddy, V. S. K., and Uthanna, S., (2007). Effect of sputtering power on the physical properties of Cu_3N films formed by DC magnetron sputtering. *Journal of Synthesis and Reactivity in Inorganic, Metal-Organic and Nano-Metal Chemistry*, **37**:393-395.

Reddy, V. S. K., Subramanyam, T.K. and Uthanna, S., (2007). Nitrogen partial pressure influence on physical properties of DC magnetron sputtered copper nitride films. *Optoelectronics and Advanced Materials*, **1**(1):31-35.

Saha, B., Das, S. and Chattopadhyay, K. K., (2007). Electrical and optical properties of Al-doped cadmium oxide thin films deposited by radio frequency magnetron sputtering. *Journal of Solar Energy Materials and Solar Cells*, **91**:1692-1697.

Santoz-Cruz, J., Torres-Delgado, G., Zuniga-Rumero, C.I., Castanedo-Perez, R. and Zelaya-Angel, O.,(2007). Optical and Electrical characterization of Fluorine doped cadmium oxide thin films prepared by the sol-gel method. *Thin Solid Films*, **515**: 5381-5385.

Serbetci, Z., Gunduz, B., Al-Ghamdi, A.A., Al-Hamzmic, F., Arik, K., El-Tantawy, F., Yakuphanoglu, F. and Farooq, W.A., (2014). Determination of optical constants of nanocluster CdO thin films deposited by sol-gel technique. *Acta Physica Polonica*, **126** (3):798-807.

Siraj, K., Khaleeq-ur-Rahman, M., Hussain, S.I., Rafique, M.S. and Anjum, S., (2011). Effect of deposition temperature on structural, surface, optical and magnetic properties of pulsed laser deposited Al-doped CdO thin films. *Journal of Alloys and Compounds*: doi:10.1016/j.jallcom.2011.03.183.

Soga, T., (2006). Nanostructured materials for solar energy conversion. Elsevier publishers, Oxford. Pages 19-32.

Suhail,M.H., Ibrahim, I.M. and Rao, G.M., (2012).Characterization and gas sensitivity of cadmium oxide thin films prepared by thermal evaporation technique. *Journal of Electronic Devices*, **13**:965-974.

Wolfang Theiss, (2012). Hard and software for optical spectroscopy: Technical maual,Aachen publisher, Germany. Pp 22-134.

Wongcharoen, N., Gaewdang, T. and Wongcharoen, T., (2012). Electrical Properties of Al-Doped CdO Thin Films Prepared by Thermal Evaporation in Vacuum. *Energy Procedia*, **15**:361 – 370.

Xing-ao, L., Jian-Ping, Y., Yong-Tao, L., Li-Xia, W. and Hai-Yun, W., (2011). Study on copper nitride thin films prepared by reactive DC magnetron sputtering. *Materials Science Forum*, **687**:706-710.

Xiu, F.X., Yang, Z., Zhao, D.T., Liu, J.L., Alim, K.A., Balandin, A.A., Itkis, M.E. and Haddon, R.C., (2006). ZnO Growth on Si with low temperature CdO and ZnO buffer layers by molecular-beam epitaxy. *Journal of Electronic Materials*, **35**(4): 691-694.

Yahiya, K.Z., (2008). Fabrication and Characterization of High Efficient CdO/SI Photovoltaic Solar Cells. *Journal of Al-Nahrain University*, **11**(1):56-58.

Yuan, X.M., Yan, P.X. and Liu, J.Z., (2006). Preparation and characterization of copper nitride films at various nitrogen contents by reactive radio-frequency magnetron sputtering. *Materials Letters*, **60**:1809–1812.

Yue, G.H., Yau, P.X., Liu, J.Z., Wang, M.X. and Yuan, X.M.,(2005).Copper nitride thin films prepared by reactive radio-frequency magnetron sputtering. *Journal of Applied Physics* **98**(103506): 1-7.

APPENDECES

Appendix 1: A photograph of Edwards 306 vacuum coater machine

Appendix 2: A photograph of UV-VIS-NIR spectrophotometer

Appendix 3: A photograph of Keithley 2400 source meter